GEAP - 3709
Informal AEC Research and Development Report

W. H. Cook

DOCKET NO. 50-10
Suppl. File cy

Stability Section.

Name as part of 9-16-61 Suppl. info on "Proposed High Power Steam Test"

FUEL CYCLE PROGRAM

A BOILING WATER REACTOR

RESEARCH AND DEVELOPMENT PROGRAM

THIRD QUARTERLY REPORT

Prepared for

THE U. S. ATOMIC ENERGY COMMISSION

Under Contract No.

AT (04-3)-189, PROJECT AGREEMENT NO. 11

GENERAL ELECTRIC

ATOMIC POWER EQUIPMENT DEPARTMENT

SAN JOSE, CALIFORNIA

FUEL CYCLE PROGRAM

A BOILING WATER REACTOR RESEARCH AND DEVELOPMENT PROGRAM

THIRD QUARTERLY REPORT

JANUARY 1961 - MARCH 1961

Prepared for

THE UNITED STATES ATOMIC ENERGY COMMISSION

Under Contract Number

AT (04-3)-189, PROJECT AGREEMENT NO. 11

By

GENERAL ELECTRIC COMPANY

Atomic Power Equipment Department

San Jose, California

ACKNOWLEDGEMENT

The Fuel Cycle Program is sponsored by the AEC and is being conducted by the General Electric Company with the following individuals contributing to the program during the third quarter.

Project Engineer	C. L. Howard*
Project Consultant	S. Levy
Fuel Development	T. J. Pashos
Fuel	W. C. Rous
Instrumented Assemblies	A. G. Dunbar
Heat Transfer and Fluid Dynamics	E. Janssen J. Kervinen
Burnout Heat Transfer Observational Boiling Experiment	F. E. Tippets
VBWR Core Analysis	
Heat Transfer and Fluid Dynamics	F. E. Tippets* C. Dunlap V. G. Grayhek T. J. Judge W. A. Sutherland
Physics Programs	D. L. Fischer J. O. Arterburn M. R. Hackney T. Tillinghast
Stability Analysis	W. H. Cook* J. M. Case R. O. Niemi
VBWR Fuel Cycle Experimental Program	C. L. Howard* J. A. Hodde C. L. Swan
VBWR Programming	E. L. Burley
VBWR Operations	J. B. Violette VBWR Staff

* Changed on March 13, 1961

LEGAL NOTICE

This report was prepared as an account of Government sponsored work. Neither the United States, nor the Commission, nor any person acting on behalf of the Commission:

A. Makes any warranty or representation, expressed or implied, with respect to the accuracy, completeness, or usefulness of the information contained in this report, or that the use of any information, apparatus, method, or process disclosed in this report may not infringe privately owned rights; or

B. Assumes any liabilities with respect to the use of, or for damages resulting from the use of any information, apparatus, method, or process disclosed in this report.

As used in the above, "person acting on behalf of the Commission" includes any employee of contractor of the Commission, or employee of such contractor who prepares, disseminates, or provides access to, any information pursuant to his employment or contract with the Commission, or his employment with such contractor.

Prepared by: J. A. Hodde

J. A. Hodde, Engineer
Engineering Development

Approved by: C. L. Howard

C. L. Howard, Project Engineer
Fuel Cycle Development Program

Approved by: D. K. Imhoff

D. K. Imhoff, Manager
Engineering Development

TABLE OF CONTENTS

		Page No.
I.	Introduction	1
II.	Summary	3
III.	Task A - Advanced Fuel Power-Limit Tests	4
	A. Task A-I Design of High Output Fuel Core	4
	1. Relationship of Voids and Flux Distributions	
	2. Axial Flux Leakage	
	3. Resonance Escape Calculations	
	4. Subcooled Voids	
	B. Task A-II Fabrication of Core	5
	C. Task A-III Instrument and Calibrate Three Assemblies	7
	D. Task A-IV Stability Tests	8
	1. Preliminary Tests	
	2. Frequency Analyzer	
	3. Analytical Data Reduction	
	4. Rod Oscillator Mechanism	
	5. Analytical Results	
	E. Task A-VI Irradiation in VBWR	18
	1. Irradiation History	
	2. Start-up Tests	
	3. VBWR Shutdown	
	4. VBWR Loading and Operating Schedules	
	F. Task A-VII Special Fuel Program	22
	1. Detailed Description of the Special Fuel Assemblies	
	2. Progress on Procurement of Material for the Special Fuel Assemblies	
IV.	Task B - Heat Transfer and Fluid Dynamics	28
	A. Task B-I Burnout Heat Transfer	28
	1. Previous Burnout Work	
	2. New Burnout Data	
	3. High-Pressure Observational Boiling Experiment	
	B. Task B-IV Two-Phase Pressure Drop	37

LIST OF FIGURES

		After Page
Figure 1	Vertical Power Distribution as a Function of Core Power	4
Figure 2	Vertical Power Distribution as a Function of Flow Rate	5
Figure 3	Reactivity as a Function of Flow Rate At Constant Power and Constant Subcooling	5
Figure 4	VBWR Vessel Internals	8
Figure 5a	Run No. 10-27-60-1	9
Figure 5b	Run No. 11-19-60-2	9
Figure 5c	Run No. 11-25-60-3	9
Figure 5d	Run No. 1-28-61-2	9
Figure 6	Cumulative Percent vs. Power, Run No. 10-27-60-1	9
Figure 7	Cumulative Percent vs. Power, Run No. 11-19-60-2	9
Figure 8	Cumulative Percent vs. Power, Run No. 11-25-60-3	9
Figure 9	Cumulative Percent vs. Power, Run No. 1-28-61-2	9
Figure 10	Run No. 1-17-61-1 Spectral Power Density	10
Figure 11	Run No's 1-28-61-1, 1-28-61-2 and 1-28-61-6	10
Figure 12	Frequency Analyzer	11
Figure 13	Rod Oscillator Mechanism	12
Figure 14	Logic Block Diagram of Reactor Analytical Model	13
Figure 15	Single-Node Hydraulics Model	13
Figure 16	Cumulative Energy Extracted from All Fuel in VBWR	18
Figure 17a	Fuel Assembly 4H after 479 MWD/T	20

LIST OF FIGURES (Continued)

		After Page
Figure 17b	Fuel Assembly 2H After 323 MWD/T	20
Figure 18	Effect of Steam Quality and Mass Flow Rate on Burnout Heat Flux	29
Figure 19a	Hydraulic Diameter Effect on Burnout for a 9-foot Heated Length	29
Figure 19b	Hydraulic Diameter Effect on Burnout for a 6-foot Heated Length	29
Figure 20a	Heated Length Effect on Burnout for 0.500 inch Hydraulic Diameter	29
Figure 20b	Heated Length Effect on Burnout for 0.335 inch Hydraulic Diameter	29
Figure 21	General View of Experimental Equipment in High Pressure Observational Boiling Experiment	29
Figure 22	Principal Parts of Observational Test Section	29
Figure 23	Observational Test Section Heater Elements Before and After Actual Burnout	30

LIST OF TABLES

		Page No.
Table 1	Breakdown of Fuel-Life Fuel Assemblies	6
Table 2	Amplitudes of Fower Fluctuations in VBWR Under Various Operating Conditions	9
Table 3	Burnup Per Assembly to January 29, 1961	18
Table 4	Specific Powers and Power Densities in Fuel Cycle Fuel	19
Table 5	VBWR Loading Schedule - Second Quarter 1961	20
Table 6	VBWR Operating Schedule - Second Quarter 1961	21
Table 7	Fuel and Cladding Placed on Order for Special Fuel Assemblies	25
Table 8	Status of Material in Special Fuel Program	26,27
Table 9	Range of Variables in the Observational Boiling Experiment	30

I INTRODUCTION

The Fuel Cycle Program is an integrated program of investigation in the Vallecitos Boiling Water Reactor (VBWR) and other facilities to improve the technological limits of boiling water reactors in the following areas:

Task A

1. Extend fuel life information on oxide fuel at high specific power operation and raise the performance limits of oxide fuels.

2. Study power stability and performance characteristics of an oxide-fueled core under natural and forced circulation to improve design limits.

Task B

1. Conduct out-of-pile experiments in heat transfer and fluid dynamics in the areas of burnout heat transfer, hydraulic instability, steam void observational studies, and two-phase pressure drop to support in-core work.

Task C

1. Study long-term reactivity characteristics of fuels having lattice characteristics of large power reactors.

2. Measure initial conversion ratio of a number of lattice configurations characteristic of large, oxide-fueled power reactors.

This report is written in partial fulfillment of contract AT(04-3)-189, Project Agreement No. 11, Fuel Cycle Program, between the United States Atomic Energy Commission and the General Electric Company. It describes the technical progress on the Fuel Cycle Program for the months of January, February and March, 1961. Prior reports to the Commission under this contract have included the following:

1. GEAP-3516, First Summary Progress Report, March 1959 - July 1960

2. Monthly Progress Letter No. 1, August 1960

3. GEAP-3558, First Quarterly Progress Report, August 1960 - September 1960

4. Monthly Progress Letter No. 2, October 1960

5. Monthly Progress Letter No. 3, November 1960

6. GEAP-3627, Second Quarterly Progress Report, October 1960 - December 1960

7. GEAP-3628, Prediction of Two-Phase Flow From Mixing Length Theory, S. Levy, December 27, 1960

8. Monthly Progress Letter No. 4, January 1961

9. Monthly Progress Letter No. 5, February 1961

II SUMMARY

Task A - Advanced Fuel Power-Limit Tests

1. The continuing analysis of the VBWR core has resulted in refinements in the calculations for reactivity in voids, flux leakage and resonance escape probability.

2. The Zircaloy cladding for 25 fuel assemblies has been received and has passed inspection. Fabrication of this fuel is to be completed by June.

3. Preliminary measurements of VBWR flux oscillations, being used to develop instrumentation and data interpretation techniques, show random normally-distributed oscillations with a predominant frequency of 0.5 to 1.0 cycles/second.

4. A model for analog computer simulation of a reactor as a feedback control system was adapted to VBWR. Equations for the hydraulics model and preliminary results from use of the model are presented.

5. Irradiation of the Fuel Cycle stainless steel clad assemblies has reached 412 MWD/T with specific powers of 28 kw/kg (average) and 52 kw/kg (peak) during January.

6. Visual examination of the fuel after this irradiation indicates that it is in good condition.

7. The VBWR was shut down during February and March for replacement of all in-core components made of Armco 17-4 PH stainless steel with 304 stainless steel.

8. The details of the first eight special fuel assemblies have been determined and materials have been ordered.

Task B - Heat Transfer and Fluid Dynamics

1. The effects of steam quality, mass flow rate, and rod diameter on burnout heat flux are shown. The burnout heat flux varies inversely with mass flow rate; this result is contradictory to several previous correlations.

2. The experimental phase of the high-pressure observational boiling experiment was completed. Reproducibility of the burnout points is good (about $\pm$ 1-1/2%). High speed movies of the flow conditions at burnout are being analyzed.

II. TASK A - ADVANCED FUEL POWER-LIMIT TESTS

A. Task A-I Design of High Output Fuel Core

This sub-task includes the analysis and design of a core-sized quantity of stainless steel and zircaloy-clad fuel for the conduct of fuel life tests in VBWR. This work also includes appropriate safeguards and core analyses, and design and coordination of test programs in VBWR.

The design of both the stainless steel and zircaloy-clad fuel is completed.

Based on the limited operating experience so far, the core calculations were found to overestimate the VBWR operating core reactivity by an average of approximately 4%. Accordingly, during the reporting period a review was made of the methods used in calculating the core reactivity. During the process, a more complete understanding of the relationships between voids, flux, flow, flow leakage and resonance escape probability has been gained. The results of this work will be applied to the core calculations and reactivity versus burnup program under Task C. In addition a body of information will be available on the interactions of flux, voids, recirculation flow and inlet subcooling which will be applied to the analytical stability work under the Fuel Cycle program.

1. Relationship of Voids and Flux Distributions

As steam voids are formed in the core of boiling water reactors, the local neutron flux is reduced because of loss of the moderator. Since the steam voids are found predominantly in the upper half of the core, the axial flux distribution is shifted from the "chopped" cosine shape to a skewed flux distribution in which the greatest power generation occurs in the lower half of the core. This effect is seen in Figure 1. Similarly the radial power distribution is affected in a similar manner by the radial steam void distribution. The experimentally determined reactivity in voids is approximately 1.5% Δk/k higher than the calculated values. This is being investigated to determine whether the difficulty is in the calculated flow and voids, or in the effective reactivity worth of the voids. Part of this difference is explained by the sub-cooled voids as discussed below.

2. Axial Flux Leakage

Another area which has been investigated is that of axial flux leakage. All VBWR core calculations to this time have assumed an axial flux leakage which would be characteristic of a pure water reflector. However, the top reflector is water, steam and steel structure and the bottom reflector consists of water and steel. An estimate was made of the effect of this assumption on the total core reactivity. The analysis indicated that the additional use of steam and steel structure in the calculations may reduce the total core reactivity by as much as 1.3%.

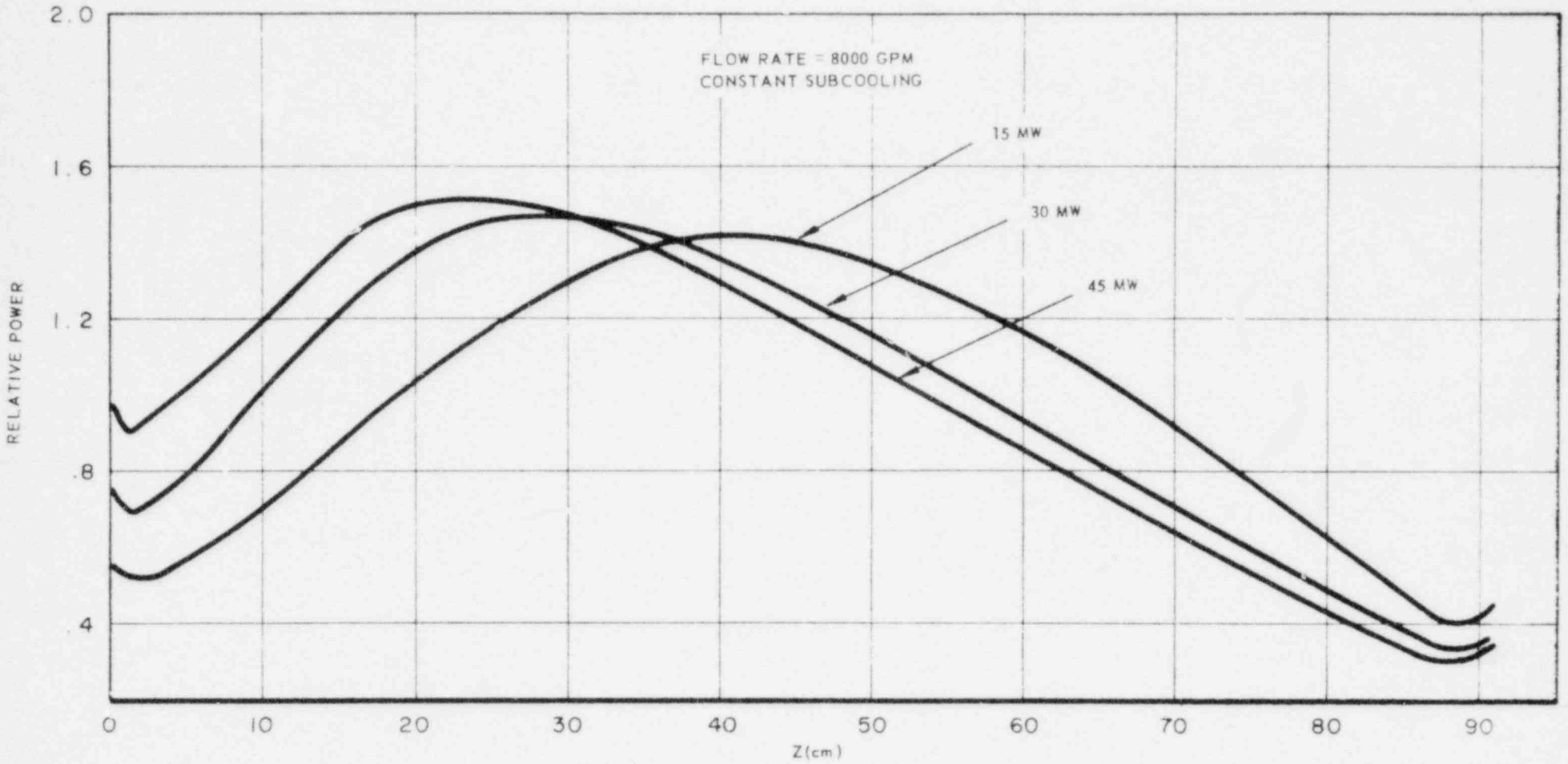

FIGURE 1
VERTICAL POWER DISTRIBUTION AS FUNCTION OF CORE POWER

3. Resonance Escape Calculations

The resonance escape was re-evaluated for the various fuel types in VBWR. These calculations used the clumped lattice method with Hellstrand's data* for the resonance integral constants. Previously the resonance escape was calculated using a unit cell geometry and other values for the constants in the resonance integral. In the unit cell geometry an individual fuel rod and the moderator in its immediate vicinity is considered. The clumped lattice model evaluates the effects of the adjacent fuel rods and moderator on the value of the resonance integral constants for that rod. Results of this analysis indicate that the resonance escape values used in previous VBWR calculations were somewhat high. The total core reactivity estimates may be reduced by 1.5% to 2% by using the new analytical approach. Approximately half of this difference is attributed to the resonance integral constants and the other half to the treatment of the fuel and moderator geometry.

4. Subcooled Voids

Previous core calculations did not include the effects of voids in the subcooled region of the core. An effort was made to evaluate this effect on the VBWR core calculations made to date. It was found that inclusion of steam voids in the subcooled region may decrease core reactivity by about 0.5%.

The combined effect of these studies showed that calculated values of core reactivity could be reduced by about 4%. Effects of varying recirculation flow rate and power level on axial power distribution have been examined under certain conditions. Figure 1 presented the vertical power distribution as a function of core power level with a constant recirculation flow and at constant subcooling. Figure 2 shows the axial power distribution as a function of flow rate for a constant power level and subcooling. These studies will be extended to examine the effects of subcooling variation on steam void and power distribution.

B. Task A-II Fabrication of Core

This sub-task includes fabrication of the fuel-life fuel assemblies. The fuel is UO_2, clad with either stainless steel or zircaloy. A breakdown of the fuel life assemblies is shown in Table I. This fuel is expected to provide information on causes of fuel failure and reactivity versus lifetime for a statistically significant quantity of fuel.

Twenty-five of the stainless steel clad assemblies were delivered to VBWR in September 1960. Fabrication of the zircaloy-clad assemblies has been delayed because of a delay in the fabrication of the zircaloy tubing for the cladding.

* Hellstrand, E, "Measurement of the Effective Resonance Integral in Uranium Metal and Oxide in Different Geometries", Journal of Applied Physics, Vol. 28, No. 12, December 1957.

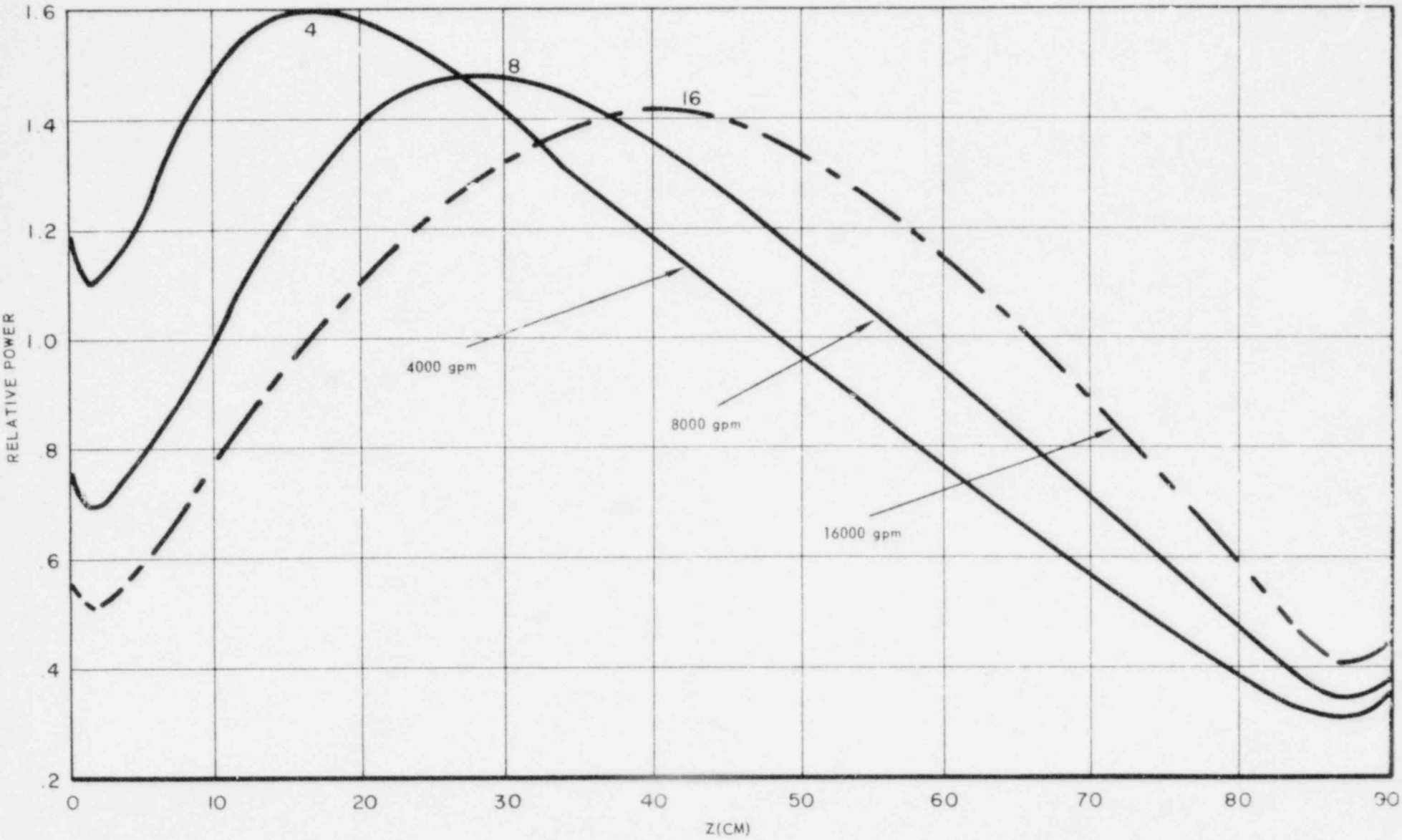

FIGURE 2
VERTICAL POWER DISTRIBUTION AS FUNCTION OF FLOW RATE
AT 30 MW & CONSTANT SUBCOOLING

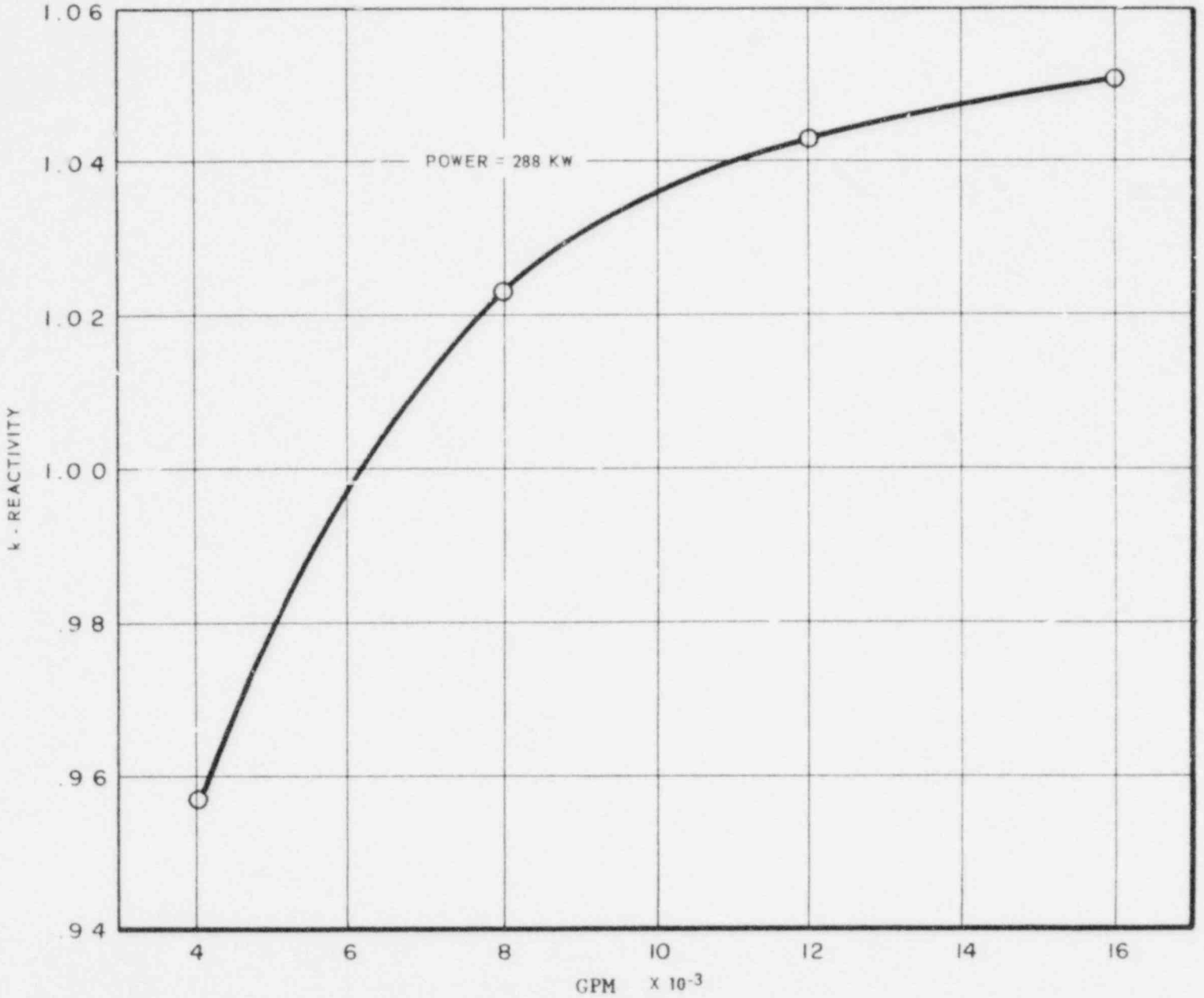

FIGURE 3
REACTIVITY AS A FUNCTION OF FLOW RATE AT CONSTANT POWER AND CONSTANT SUBCOOLING

TABLE 1

Breakdown of Fuel Life Fuel Assemblies

Fuel Assembly Designation	No. of Rods	Clad Material	UO_2 Enrichment	No. of Assemblies A-1*	A-2*	Total	Remarks
Type-H	16	304 S.S.	2.7%	10	0	10	These 10 assemblies are fuel followers
Type-I	16	304 S.S.	3.2%	8	8	16	One of the A-1 assemblies in this group has been designated as an instrumented assembly and is being fabricated under sub-task A-III.
Type-J	16	Zircaloy-2	2.7%	17	6	23	Two of the A-1 assemblies in this group have been designated as instrumented assemblies and are being fabricated under sub-task A-III
Type-K	16	Zircaloy-4	2.7%	1	1	2	
Type-J	16	Zircaloy-2	2.7%	9	5	14	Scheduled for fabrication in fiscal 1962; may be deleted from program.
Type-K	16	Zircaloy-4	2.7	2	0	2	Scheduled for fabrication fiscal 1962; may be deleted from program.
				57	20	67	

NOTE: The A-1 assemblies are fuel for the irradiation life tests and serve as "drivers". The A-2 assemblies are "reference" fuel having individually removable fuel rods to permit detailed examination.

A portion of the zircaloy-2 tubing was processed through the annealing, third and fourth drawing steps and straightening operation during January 1961. It was subsequently inspected by the vendor and shipped to San Jose, California in February 1961. Of the 2633 feet of zircaloy-2 tubing on order, approximately 2,000 feet have been delivered in the form of 40-inch lengths (i.e., 605 pieces in 40 inch lengths). Approximately 113 feet of zircaloy-4 tubing (34 pieces in 40 inch lengths) has been delivered. The inspection results for the tubing were as follows:

	Zircaloy-2	Zircaloy-4
Pieces delivered	605	34
Rejects - dimensional and visual examination	46	0
Rejects - ultrasonic examination	126	6
Available for fabrication and destructive testing	433	28

Therefore, the tubing is sufficient for the fabrications scheduled for completion in June, 1961.

23 16-rod assemblies of Zr-2 clad.

2 16-rod assemblies of Zr-4 clad (with Zr-2 to complete the assembly)

25

C. Task A-III Instrument and Calibrate Three Assemblies

Three fuel assemblies are being fabricated with temperature, flow, pressure and neutron flux instrumentation. This equipment will be installed in VBWR for the stability and performance tests. The system consists of the instrumented fuel assemblies, instrument leads which will penetrate the reactor vessel and pass to a switching center, and readout panels located in the VBWR control room. The instrument readout panels and switching center will be shared by the Fuel Cycle and High Power Density Research and Development programs.

The design of the assemblies was completed in December 1960. During the reporting period, fabrication of the readout and back-pressure panels was completed. Preparations were made at the VBWR site to install the instrument panels and provide reactor pressure vessel and enclosure penetrations. All instrumentation is either on order or has been received. The major item of work remaining on the instrumentation is the fabrication of the turbine-type flowmeters. This work will begin during April, 1961. Task A-III is approximately 80 percent completed.

D. Task A-IV Stability Tests

Power stability experiments will be conducted in September or October, 1961. They will include rod oscillation tests and operational transient experiments. They are expected to be run under natural and forced circulation conditions and may be done with dual cycle operation. Simultaneously, an analytical study of boiling water reactor stability will be carried on to predict and generalize on the results of the tests and to apply them to as large an area of boiling water reactors as possible.

1. Preliminary Tests

Preliminary power oscillation data has been obtained in VBWR under a variety of operating conditions, flows and power levels during the VBWR start-up tests. The objectives for performing these preliminary tests are:

a. To provide an experimental basis for evaluating the analytical stability work under the Fuel Cycle program.

b. To provide an opportunity to develop and perfect the experimental and data handling techniques to be used in the intensive reactor performance tests during fiscal year 1962.

The investigations so far have led to two methods for obtaining the "spectral power density" of reactors. The spectral power density is a plot of amplitude of oscillation as a function of frequency. They have shown that a resonance exists in the range of frequencies and under the conditions investigated. The investigations have also led to statistical representations of the amplitude of oscillation under various reactor conditions.

Preliminary data have been obtained under the following reactor conditions:

a. Natural circulation with baffle doors open, channel plugs out, and without orificing.

b. Forced circulation with baffle doors open, channel plugs out and without orificing.

c. Forced circulation with baffle doors closed, channel plugs in place, with or without orificing.

The location of the baffle doors is shown in Figure 4. The core layout for the preliminary tests was shown in Figure 2 of the Second Quarterly Progress Report for the Fuel Cycle Program, GEAP-3627. It is significant that a two-region core was used for the preliminary tests. The central region had a relatively tight fuel lattice (25 rods per assembly) and a 2:1 water-to-fuel ratio. The outer region of the core, containing the Fuel Cycle fuel assemblies, used 9 and 16 rod assemblies with a 4:1 water-to-fuel ratio. During the

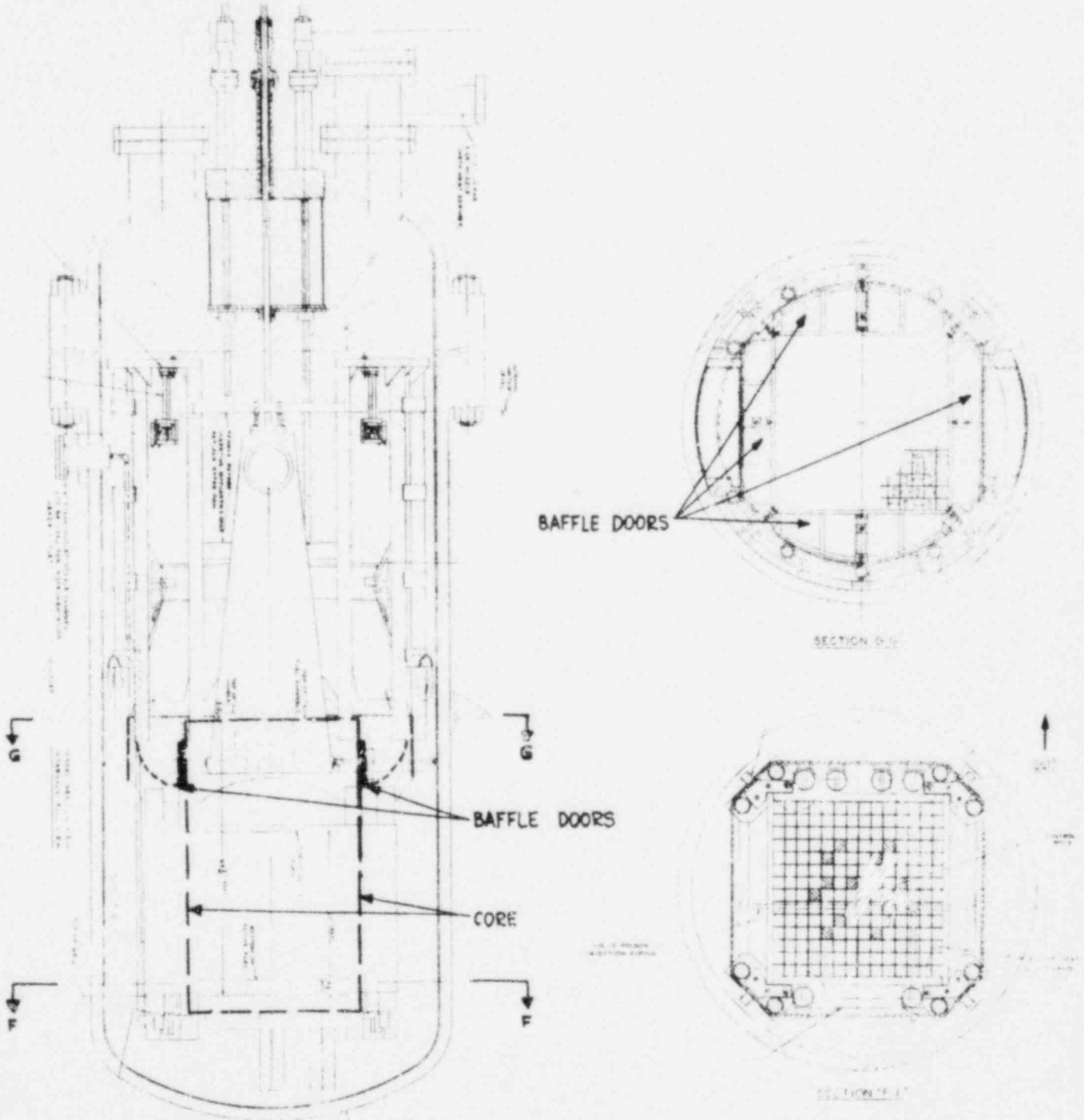

Figure 4

VBWR Vessel Internals

intensive reactor performance tests the reactor may contain both a uniform core and a two-region core.

Table 2 presents data obtained at varying reactor conditions by opening and closing the baffle doors, by inserting plugs in the unused channels surrounding the core, and under natural and forced circulation operation.

TABLE 2

Amplitudes of Power Fluctuations
in VBWR Under Various Operating Conditions

Run No.	Reactor Configuration	Power Level	Amplitude*
10-27-60-1	Natural circulation, baffle doors open, channel plugs out, no orificing	11.2 MWT	8.1%
11-19-60-2	Forced circulation, baffle doors open, channel plugs out, no orificing. Recirculation flow rate 10,200 gpm	9.1 MWT	7.5%
11-25-60-3	Forced circulation, baffle doors closed, channel plugs in, no orificing. Recirculation flow rate 10,000 gpm	10.8 MWT	5.4%
1-28-61-2	Forced circulation, baffle doors closed, channel plugs in with orificing. Recirculation flow rate 12,700 gpm	15.8 MWT	3.8%

* The amplitude is given as zero-to-peak oscillations as a percent of the reactor power.

The data obtained during the start-up tests gives the expected indications that amplitude of oscillation is decreased by (1) lower reactor power, (2) closing core bypass flow areas, (3) forced circulation and (4) higher circulation flow. Additional data is required to confirm these trends and to find the functional relationships. The future data should show lower amplitudes of oscillation because smaller orifices have been installed and core bypass leakage has been reduced during the reactor shutdown in February and March.

The amplitudes in Table 2 were obtained by the following procedure. A high speed recorder trace of the power oscillation was obtained. A portion of the trace spanning ten seconds in time was selected. For this portion of the trace 100 consecutive data points were selected which were separated by a 0.1 second interval. A histogram of the distribution of the points was drawn. A test whether the points were normally distributed, and a plot of the points was made on probability

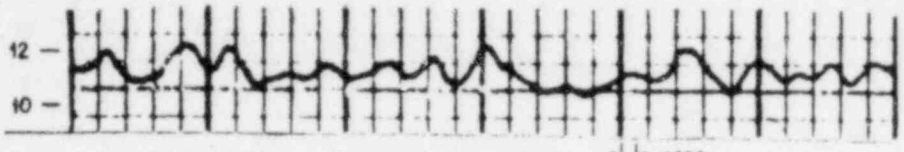

Figure 5a Run no. 10-27-60-1

Natural circulation operation with baffle doors open, channel plugs out and with no orificing

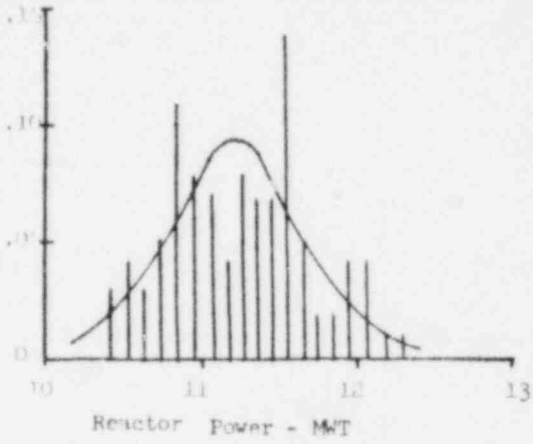

Figure 5b Run no 11-19-60-2

Forced circulation operation with baffle doors open, channel plugs out and with no orificing. Recirculation flow rate 10,200 gpm.

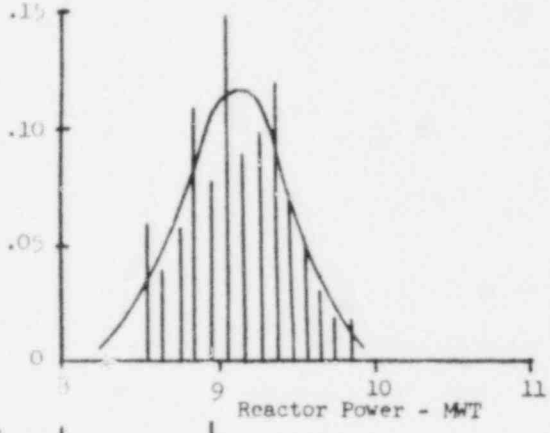

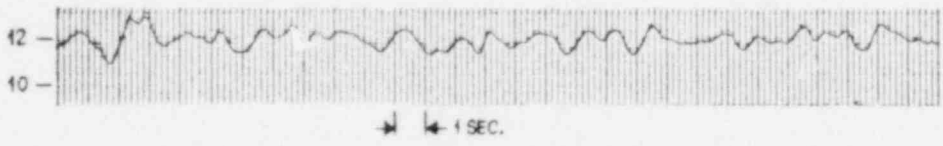

Figure 5c Run no. 11-25-60-3

Forced circulation operation with baffle doors closed, channel plugs in place and with no orificing. Recirculation flow rate 10,000 gpm.

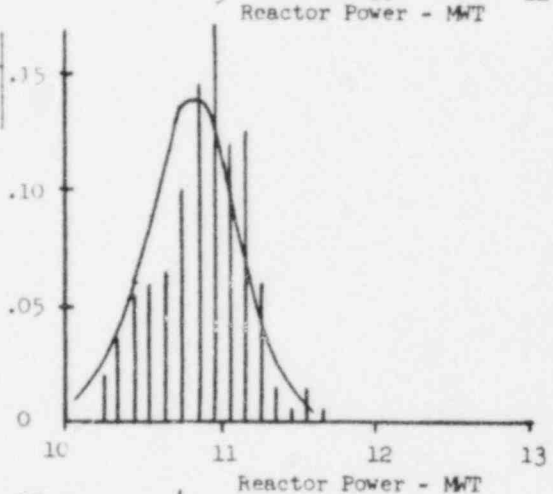

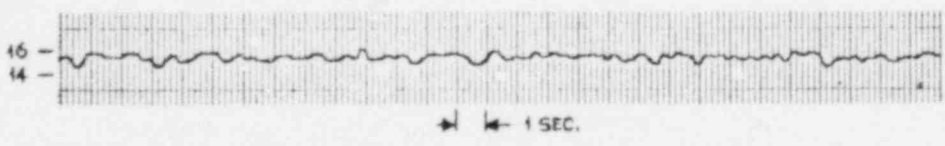

Figure 5d Run no. 1-28-61-2

Forced circulation operation with baffle doors closed, channel plugs in place and with orificing. Recirculation flow rate 12,700 gpm.

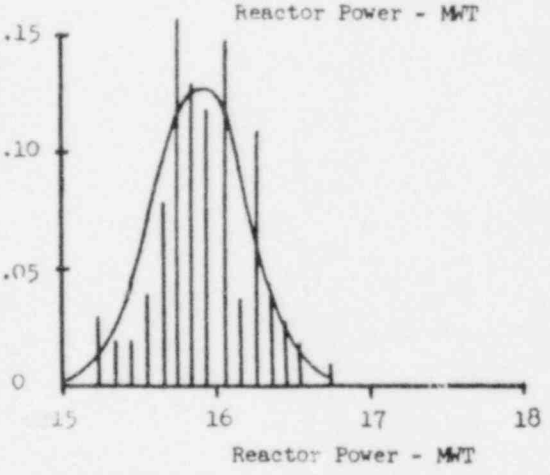

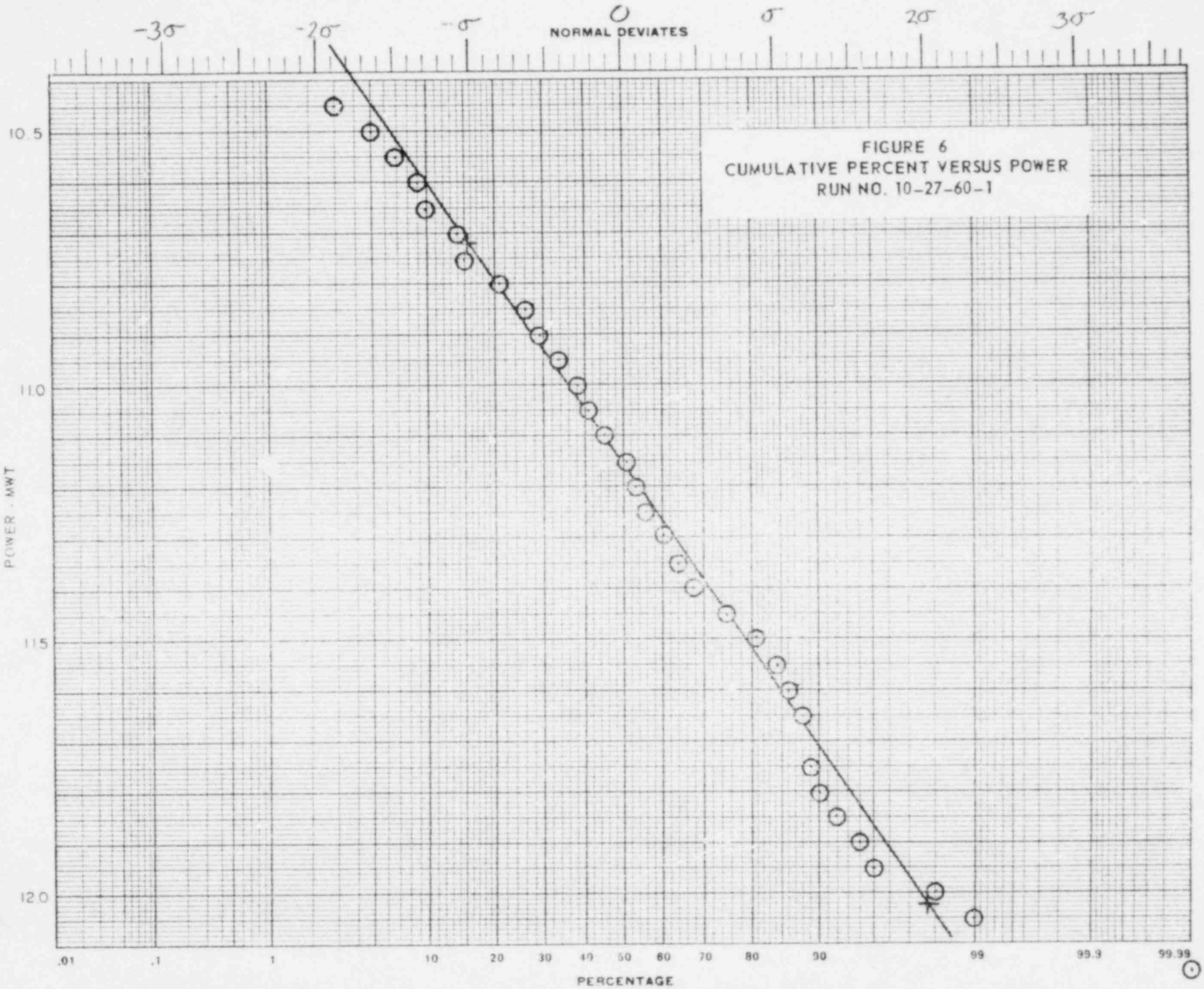

FIGURE 6
CUMULATIVE PERCENT VERSUS POWER
RUN NO. 10-27-60-1

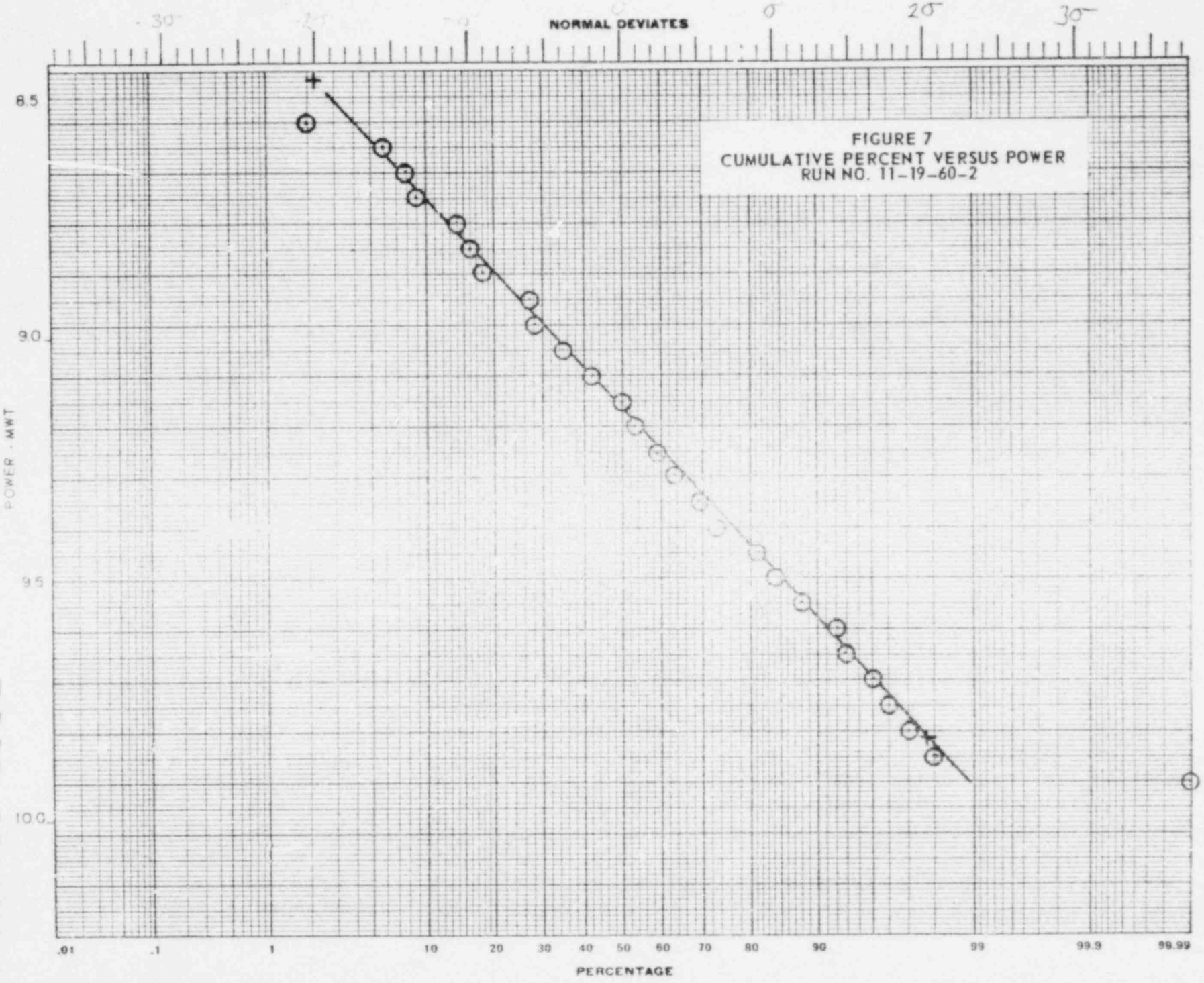

FIGURE 7
CUMULATIVE PERCENT VERSUS POWER
RUN NO. 11-19-60-2

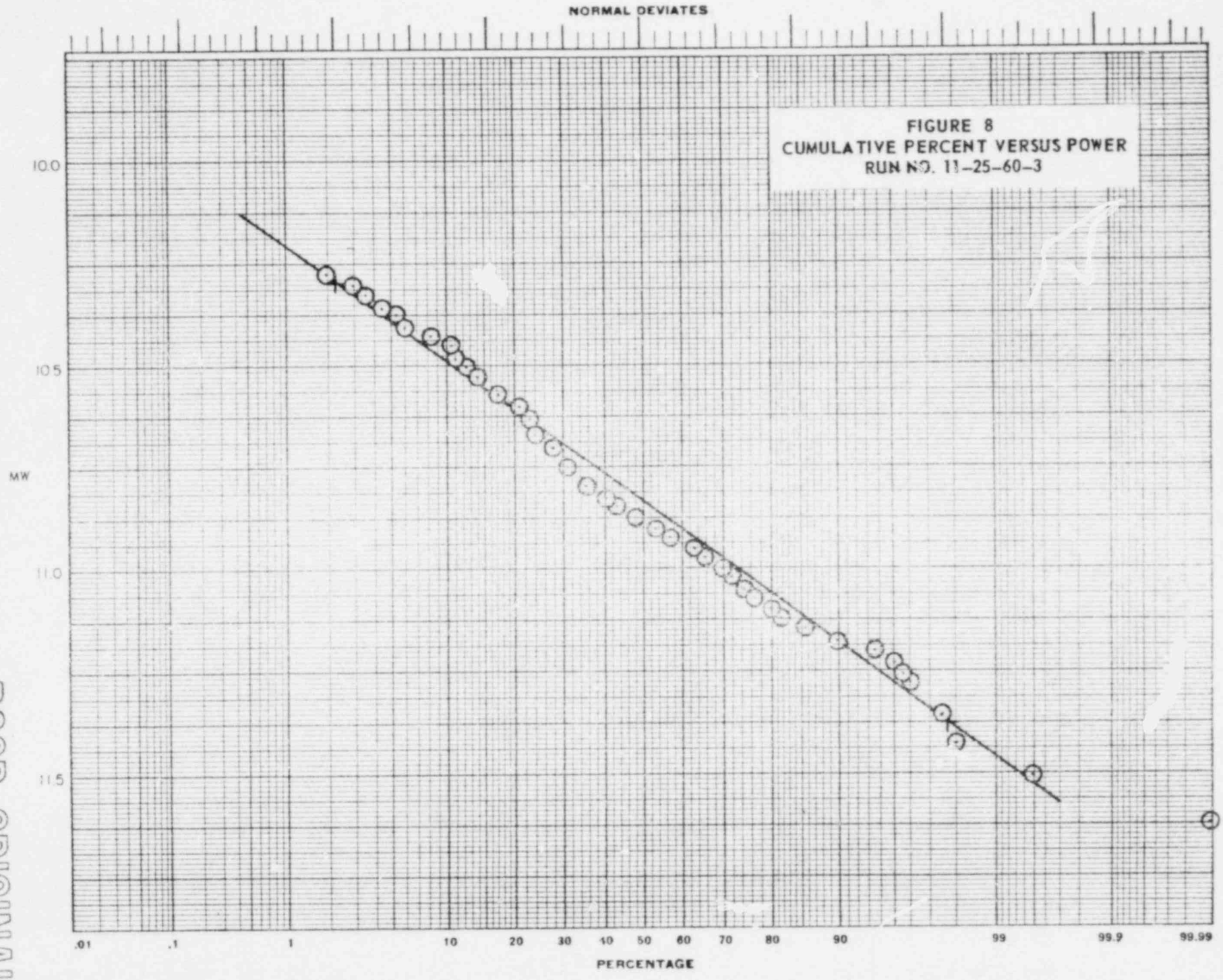

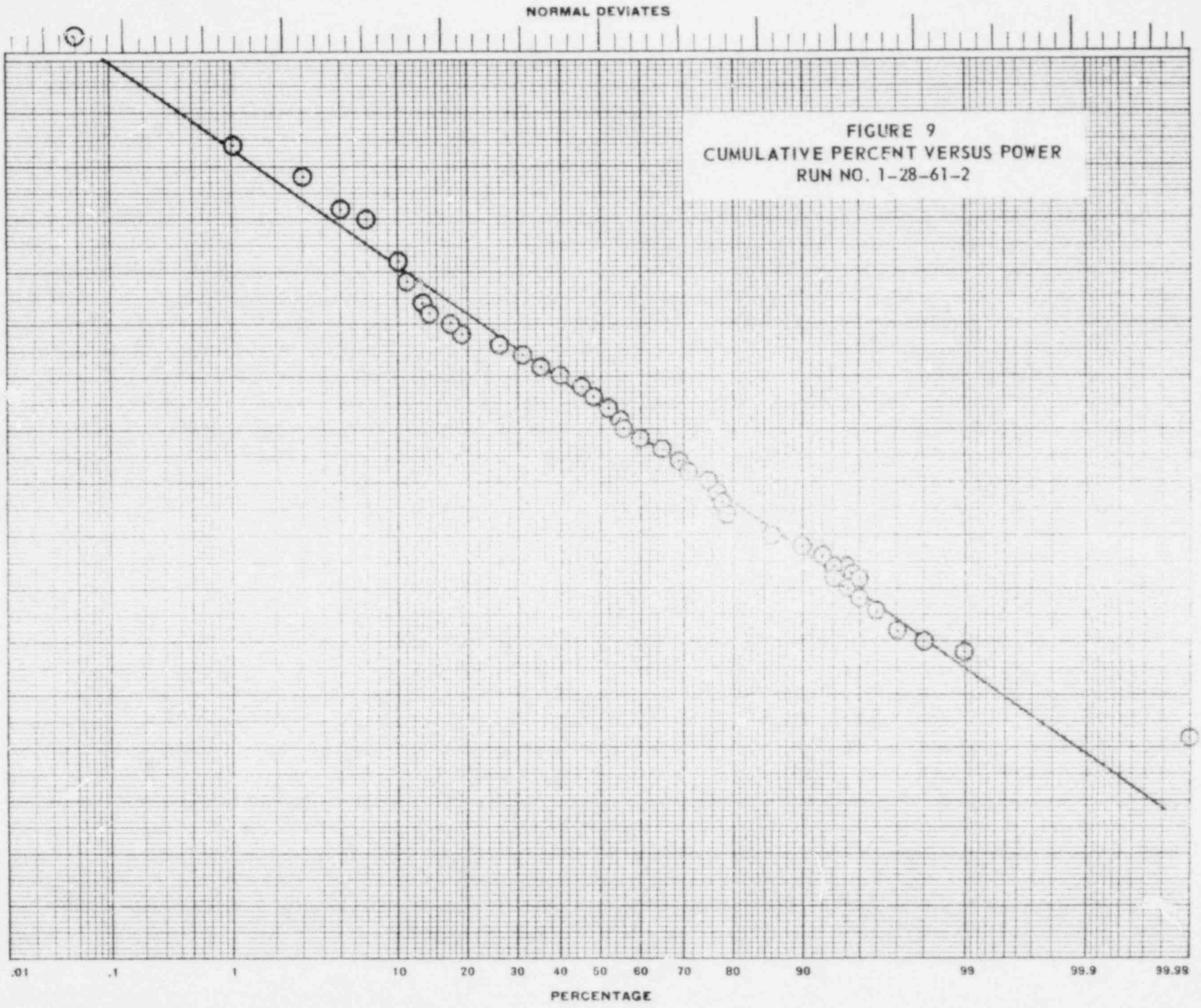

paper.* These plots are shown in Figures 6, 7, 8 and 9. The mean or most probable value and the standard deviation can be obtained directly from the cumulative percent plots. Figures 5a through d show the actual recorder traces and the histograms for the four runs in Table 2. The theoretical normal, or Gaussian, distributions are superimposed on the histograms for comparison. If the number of data points selected for the histograms were increased indefinitely, it is expected that the envelope of the histogram would approach the theoretical curves shown in Figure 5.

The zero-to-peak values for the amplitudes of the power oscillations given in Table 2 were arbitrarily taken equal to the value of 2σ, or twice the standard deviation. This includes approximately 95.4 percent of all of the data points obtained from the traces.

From superficial examination of the traces in Figure 5 it is not at all obvious what relationship exists between the frequencies and amplitudes of the power oscillations. Fortunately certain statistical techniques and electronic averaging methods may be applied to the oscillations to determine what the relationship is. These techniques will be described below.

Figures 10 and 11 present the best fit curves of measurements made with the frequency analyzer described below. The curves in Figures 10 and 11 are called the "spectral power density" of the random oscillations. They show the way in which the average amplitude of power fluctuations varies with frequency. The measurements for Figure 10 were made at 11.6 MWT and for three different flow rates: 8,000, 11,000 and 12,200 gpm. Similarly, Figure 11 presents the best fit curves of measurements made at 12,700 gpm flow rate and at 11.1, 15.3 and 19.8 MWT. In both of these figures a resonance occurs between 0.1 and 1.0 cycles per second. The resonant frequency and amplitude appears to be effected by both reactor power and recirculation flow rate, however, the data in Figures 10 and 11 does not cover a broad enough span of powers and flows from which to draw firm conclusions.

Plans have been made for extending the range of measurements to higher powers and higher flows during the remainder of the VBWR start-up tests.

An in-core ion chamber has been built for insertion into one of the stainless steel clad fuel assemblies in VBWR. It will be used during the remainder of the preliminary tests. The equipment includes the ion chamber and a flux wire tube for calibration of the ion chamber. Both the flux wire tube and the ion chamber will be inserted into a dummy rod in the fuel assembly. A guide tube and a vessel flange penetration has been provided to contain the instrument leads in the reactor.

---

* Probability paper gives the standard deviate, σ, versus the measured variable with both axes being linear. When cumulative percentage is shown on the same plot as in figures 6, 7, 8 and 9, a non-linear cumulative percentage scale results which is symmetric about the 50th percentile. A normally (Gaussian) distributed set of data points, when plotted on probability paper, will fall in a straight line.

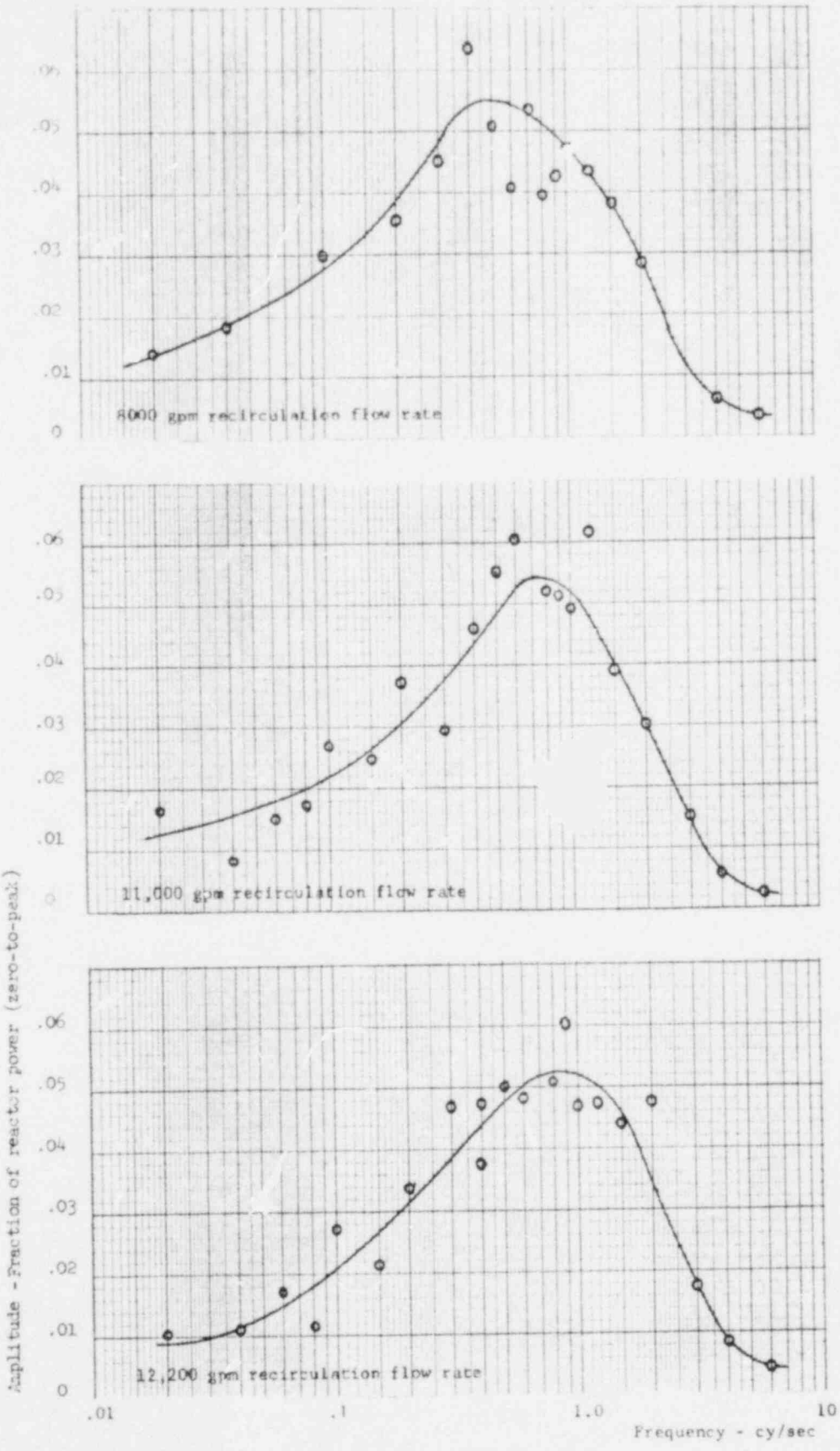

Figure 10

Run No. 1-17-61-1 Spectral Power Density Forced circulation operation with baffle doors closed, channel plugs in place and with orificing. Power level 11.6 MWT.

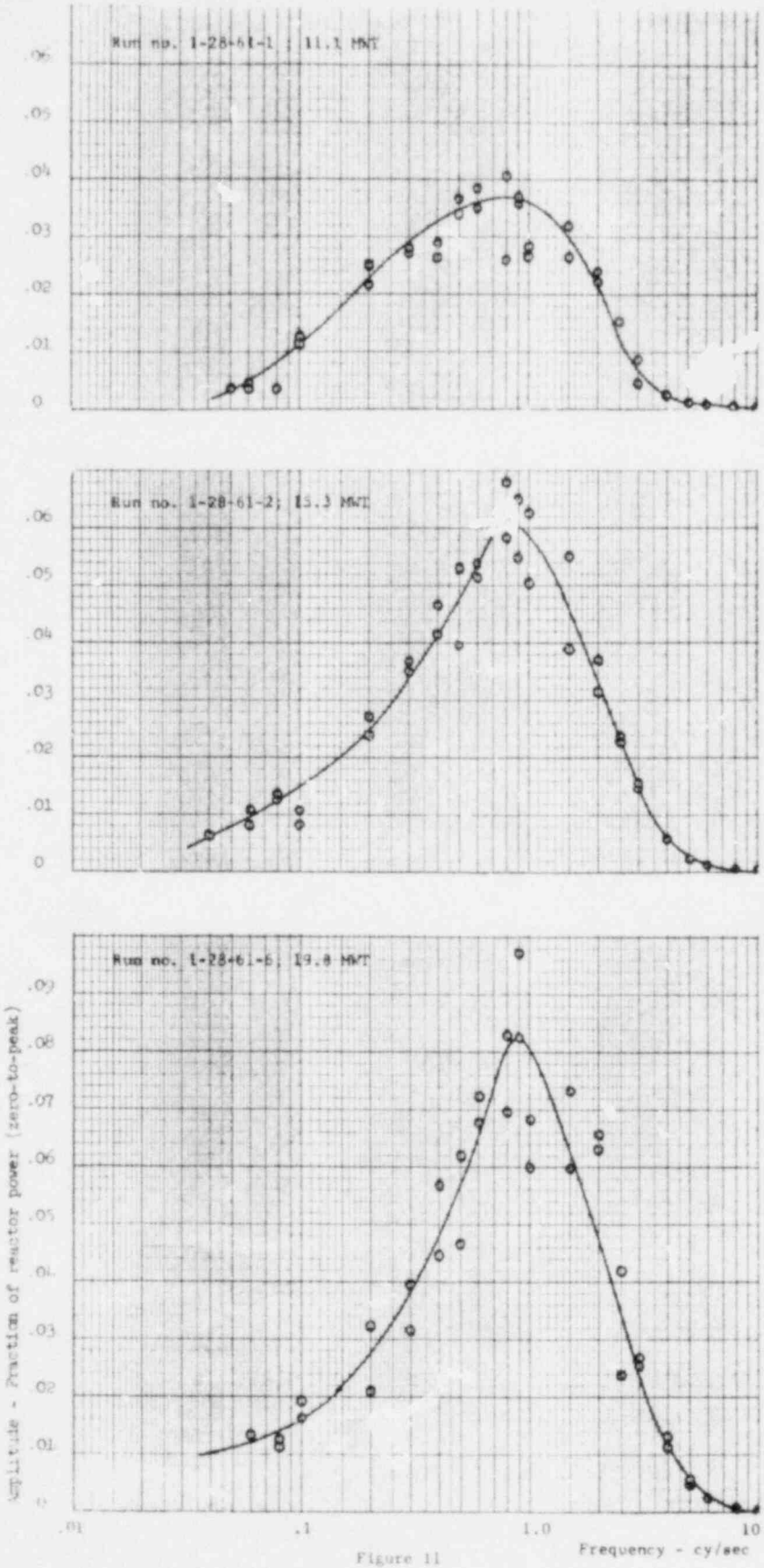

Figure 11

Run No's 1-28-61-1, 1-28-61-2 and 1-28-61-6
Spectral Power Density
Forced circulation operation with baffle doors closed, channel plugs in place and with orificing. Recirculation flow rate 12,800 gpm.

2. Frequency Analyzer

To obtain the data for Figures 10 and 11 the frequency analyzer, shown diagrammatically in Figure 12 was used. The flux level was monitored by means of an out-of-core ion chamber located approximately half way between the top and bottom of the core. The signal was fed through a 60 cycle electrical noise filter and an amplifier to a Kronhite band-pass filter. Here all but one of the frequencies of the reactor noise were filtered out. The remaining signal being analyzed was amplified and rectified in a full-wave rectifier. Then the average amplitude of this frequency was obtained by means of a voltage integrator. At least ten cycles of oscillation were used to average the amplitude of each frequency. The range investigated was between 0.01 and 10 cycles per second. In many cases two points were obtained at each frequency to get an estimate of the data scatter involved in the measurements. The greatest data scatter appears in the frequency interval between 0.1 and about two cycles per second. Note that the resonant frequency lies in this interval. Further tests are planned to determine whether this scatter is a function of measurement errors, or whether the power oscillations vary in average amplitude near the resonant point.

3. Analytical Data Reduction

The locations and amplitudes of the resonant points were difficult to determine from the data shown in Figures 10 and 11 because of data scatter. However, a statistical technique is available by which the curves of Figures 10 and 11 may be mathematically obtained from the data. This technique requires that high speed recorder traces of the flux be obtained. Punched computer cards are then made of the trace at an appropriate interval of time, every 0.05 second for example. However, it is necessary that the time interval be chosen so that it does not occur in the frequency interval of interest for the analysis. Moreover, the time interval chosen must be frequent enough so as to include all of the oscillations. By the use of a computer code the autocorrelation function of the flux trace may be obtained. The spectral power distribution (or amplitude versus frequency) may be obtained by taking the Fourier transform of the autocorrelation function.* Formally, the autocorrelation function is:

$$\phi(\tau) = \lim_{T \to \infty} \frac{1}{2T} \int_{-T}^{T} y(t) \cdot y(t + \tau)\, dt \qquad (1)$$

where $\phi(\tau)$ = autocorrelation function
$2T$ = time interval analyzed on the flux trace - seconds

* For mathematical basis see J. A. Thie, "Statistical Analysis of Power Reactor Noise", Nucleonics, October 1959, p. 102, or M. M. Moore, "A Determination or Reactor Transfer Functions from Measurements at Steady Operation", Nuclear Science and Engineering, 3, 387-394, (1958)

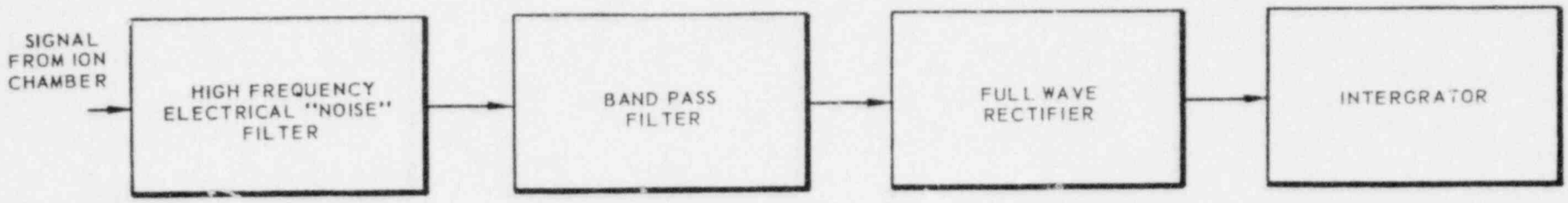

FIGURE 12
FREQUENCY ANALYZER

$y(t)$ = instantaneous reactor flux level at time t.
τ = autocorrelation interval - seconds

In terms of the digital computer the autocorrelation process consists of taking the punched computer data cards containing, say, 400 consecutive, equally spaced data points. All of the data points are superimposed upon themselves, and the ordinate value of each data point is multiplied by its superimposed counterpart. The resulting products are summed and the total is averaged over the time interval, 2T, of the trace. Then, the curves are displaced by an interval τ, 2τ, 3τ, etc. and the process is repeated at each displacement.

It is thought that a more accurate estimate of the resonant frequency and amplitude can be obtained by means of this statistical approach.

During the reporting period an autocorrelation code was prepared to apply to the reactor noise data. The code is being "debugged" for production use.

4. Rod Oscillator Mechanism

Part of the stability tests to be run in VBWR during fiscal 1962 will be control rod oscillator tests. These tests will give data on boiling water reactor response to a cyclically varying reactivity signal. The signal will be obtained by mounting a rod oscillator mechanism on one of the control rods.

The finished mechanism is pictured in Figure 13. It consists of a frame which will be mounted to the control rod drive system. A hydraulic cylinder is mounted on the frame which drives an oscillator arm. The oscillator arm provides the driving force to oscillate the control rod. The returning force is provided by the operating air pressure in the control rod drive system. Fabrication of the rod oscillator mechanism and drive system was completed during the reporting period. The mechanism and system will be tested in the General Electric control rod drive testing facility before the start of the rod oscillator test.

5. Analytical Results

Introduction

An analytical hydraulics model which had previously predicted the performance of non-nuclear boiling heat transfer loops was used to predict the reactor behavior. This model is hydraulic and thermodynamic in nature. The hydraulics model is one component of a nuclear-thermal-hydraulic feedback network model of the reactor system which was composed of

1. hydraulics model
2. fuel model
3. reactor kinetics model
4. reactor voids to reactivity conversion model

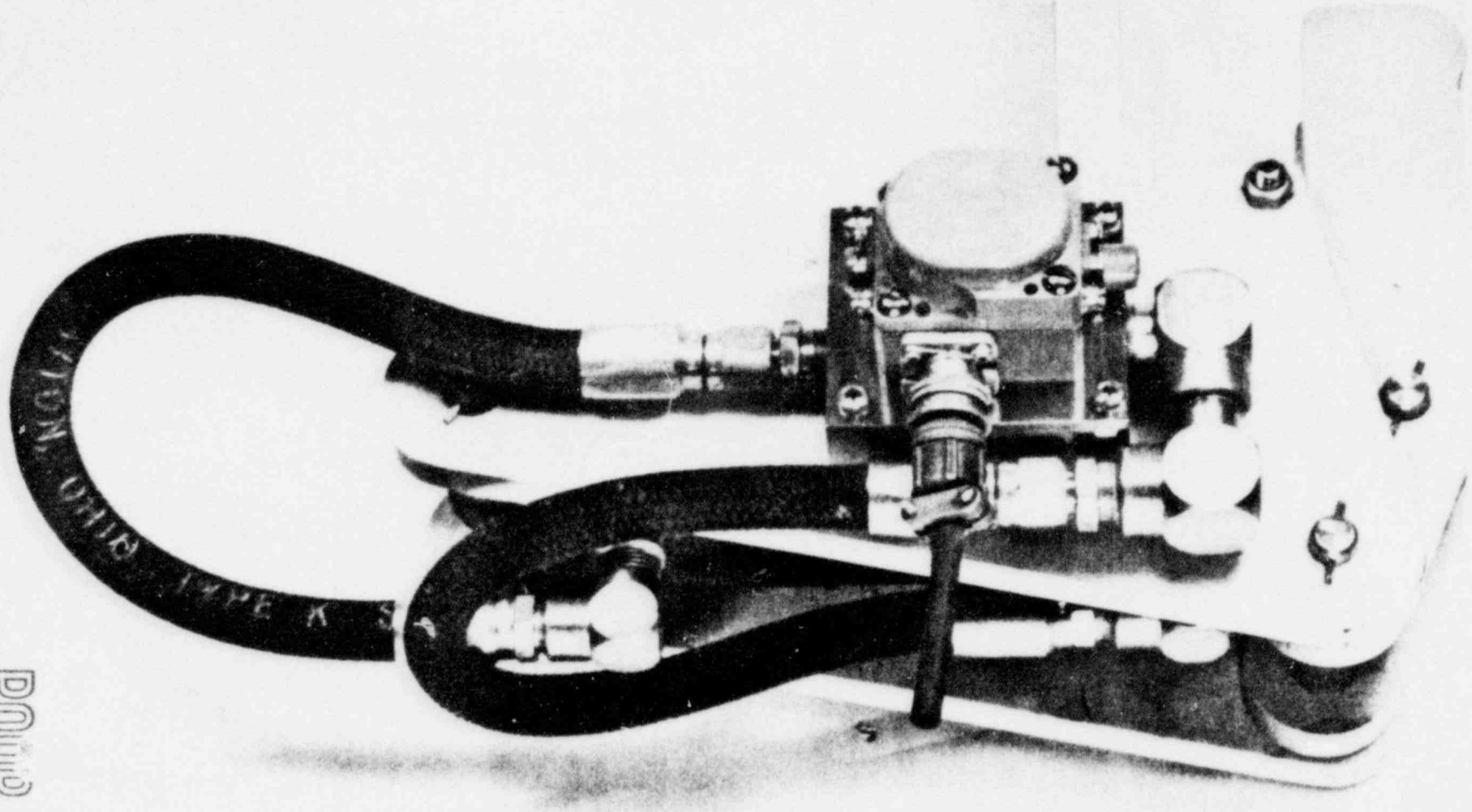

FIGURE 13

The logic block diagram for this reactor analytical model is shown in Figure 14. The fuel model, reactor kinetics model, and voids to reactivity conversion model are relatively simple and straightforward. The fuel model duplicates the time delay of fission heat generation in the fuel by thermal neutrons to be conducted through the fuel and cladding to the coolant. The reactor kinetics model is based on a conventional kinetics simulation of six groups of delayed neutrons. The voids to reactivity conversion model is simply the expression of either calculated void coefficient of reactivity or preferably measured data. In this case a calculated value was used.

The hydraulics portion of the feedback network is the distinguishing feature of the analytical model, and is described in Reference (a). It has its origin in the principles which were developed for the steady-state calculation of two-phase flow[b]. These principles were broadened to include the transient behavior of vertical two-phase flow[c] and the resulting analytical model has produced predictions which correspond well with experimental data[d]. Initially the transient analytical model was confined to only natural circulation solutions. During the course of this investigation, however, the model was modified to accept forced circulation problems.

Hydraulics Model

The transient two-phase flow model is based on an analysis which was developed for the description of a single node natural circulation loop[c]. In this single node model, shown in Figure 15, the heat is added at a single point, the initial boiling boundary. The vertical lengths in the system are important in the gravity head terms while the total lengths are important in the inertia terms.

The analysis can be described by a system of six (6) equations (given below) which are established on the basic physical principles of momentum, energy and continuity. In particular, the relationship of steam voids to quality is not based on steady state data correlations of steam voids to quality, steam to velocity ratios, or steam velocity and water velocity differences. The steam to water velocity relationship is derived from basic momentum principles and should, therefore, be capable of more accurate description of transient processes than empirical correlations of steady-state experimental data. The quality, voids, and steam and water velocities are related through the continuity equation.

(a) Case, J.M. "Neutron and Parallel Flow Channel Coupling Effects on the T-7 Flux Trap Reactor" GEAP-3508.

(b) Beckjord, E.S. and Harker, W.H. "The Steady-State Calculation of Vertical Two-Phase Flow" GEAP-3261.

(c) Beckjord, E.S. "The Stability of Two-Phase Flow Loops" GEAP-3493.

(d) Quinn, E.P. and Case, J.M. "Natural Circulation Loop Performance at 1000 psia Under Periodic Accelerations" GEAP 3397, Revision 1.

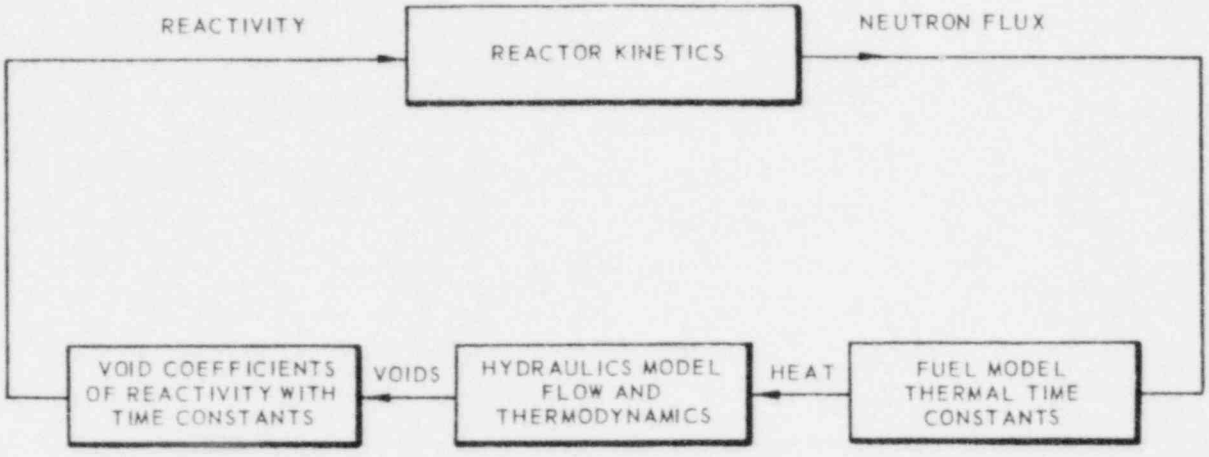

FIGURE 14
LOGIC BLOCK DIAGRAM OF REACTOR ANALYTICAL MODEL

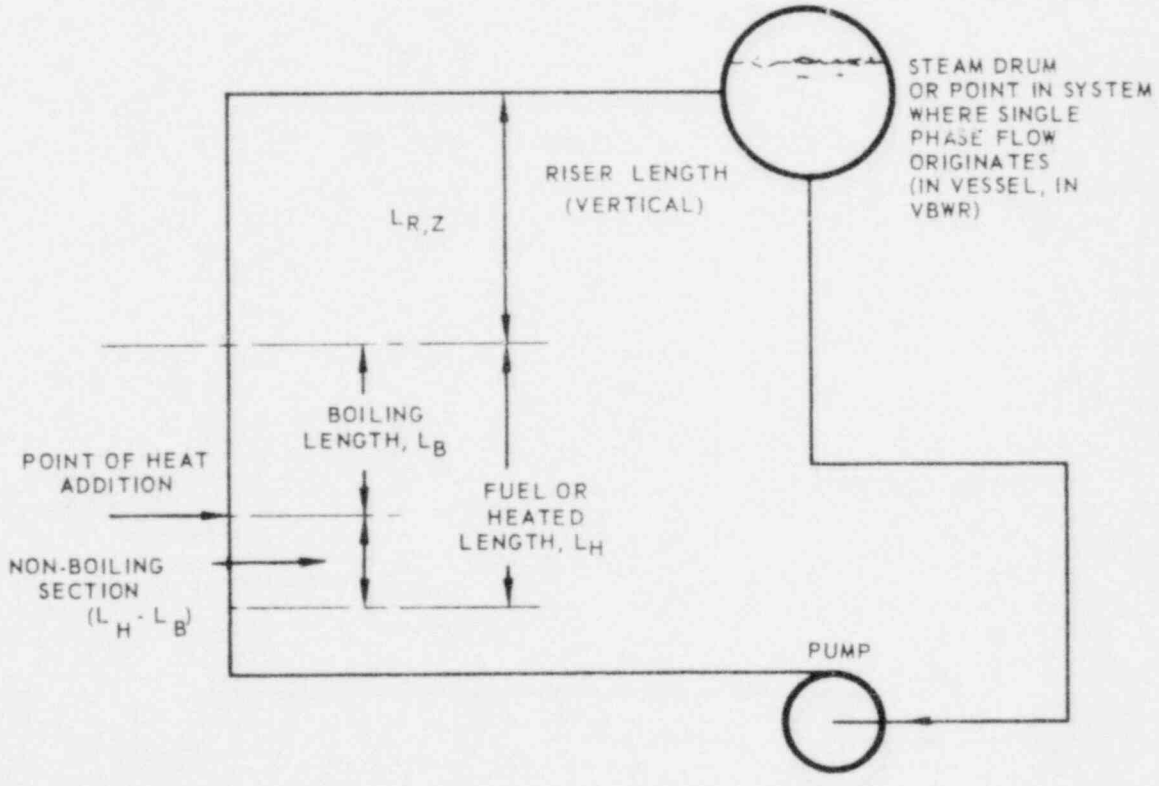

FIGURE 15
SINGLE NODE HYDRAULICS MODEL

Five of the six equations are applied directly to a description of the flow behavior in the two-phase region of the loop and the remaining equation relates the pressure contribution of the downcomer or external loop to that of the two-phase region.

The equations are:

Momentum-steam phase (Steam velocity-water velocity relationship)

$$\pi + F_{WS} \frac{(S-W)^2}{2} \left(1 - x + \frac{x}{\beta}\right) = 0 \qquad (2A)$$

Momentum - Combined Steam and water phases

$$\pi + \left(\frac{1 - R(1-\frac{1}{\beta})}{L_{RZ} + L_B} W^2 - V^2\right) +$$

$$+ \left(\frac{L_R + L_B}{L_{RZ} + L_B}\right)\left(\left[1 - R(1-\frac{1}{\beta})\right] \frac{dW}{dt} - \frac{dR}{dt}\left[W(1 - \frac{1}{\beta})\right]\right) + \qquad (3A)$$

$$+ (1 - R)g + \frac{W^2}{2}\left[\frac{F_{WR} L_R + F_{W,B} L_B + K_R}{L_{R,Z} + L_B}\right](1-R^3) = 0$$

Volume condition at point of heat addition ($x = 0$) (Combination of energy and continuity)

$$R (S-W) + W = V (1 + \alpha - \alpha\beta) + (\beta - 1)\gamma \qquad (4A)$$

Water volume condition at point of heat addition ($X = 0$) (Combination of energy and continuity - alternate form)

$$(1 - u) W = V(1 + \alpha) - \gamma \qquad (5A)$$

External loop pressure equation (Friction ... momentum)

$$\pi + g - \frac{V^2}{2}\left[\frac{K_D + K_H + F_{WD} L_D + F_{WH} (L_H - L_B)}{L_{RZ} + L_B}\right] \qquad (6A)$$

$$-\left[\frac{(L_D + L_H - L_B)}{L_{RZ} + L_B}\right] \frac{dV}{dt} = 0$$

Time delay, relationship of average void fraction to void fraction at boiling boundary. This is also a measure of the transit time of a void variation across the two-phase section

$$R = \frac{1}{L_{RZ} + L_B} \int_0^{L_{RZ} + L_B} U \, dx \qquad (7A)$$

In Laplace transfer form

$$\frac{R}{u} = \frac{1-e^{-\mu}}{\mu} \quad \text{where } \mu = \text{complex Laplace operator}$$

or approximately:

$$\frac{d^2R}{dt^2} + \frac{6}{T}\frac{dR}{dt} + \frac{12}{T^2} R = \frac{12}{T^2} U$$

where:

η = Average two-phase pressure gradient divided by liquid density, $\frac{1}{\rho_w}\left(\frac{\Delta P}{\Delta L}\right)$

S = Average steam velocity, feet per second

W = Average water velocity, feet per second

V = Inlet velocity at fuel element, feet per second

α = Subcooling factor = $\frac{h_w - h_{sc}}{h_{fg}}$ = $\frac{\text{subcooling enthalpy}}{\text{vaporization enthalpy}}$

β = ρ_s/ρ_w = ratio of steam to saturated water density

γ = Heat factor = $\frac{Q}{A\rho_w h_{fg}}$ = heat input per unit flow area divided by product of water density and vaporization enthalpy.

u = Void fraction at boiling boundary after heat input

R = Average void fraction in two-phase section

t = Time, seconds

T = Transit time of void fraction change from point of heat input to exit

L_D = Length of downcomer (external loop) feet

L_H = Length of heated section (fuel), feet.

L_B = Length of boiling section, feet

L_R = Length of riser, feet

L_{RZ} = Vertical length of riser, feet

x = Quality, percent

K_D = Sum of loss coefficients in downcomer or external loop, expressed relative to velocity V.

K_H = Sum of loss coefficients in single phase section of heated section.

F_{ws} = Shear coefficient relating drag between steam and water phases.

F_{WD} = Friction factor in downcomer or external loop relating friction pressure drop in terms of velocity, V.

F_{WH} = Friction factor in single phase heated region relating pressure drop to velocity, V.

The six equations which comprise the hydraulics model are non-linear in form. Loop flow dynamics can be investigated for small disturbances about the steady-state condition, by the linearization and normalization of these non-linear equations. The solution of these equations yields the variables in terms of percent of steady-state values. The normalized and linearized equations have the following form:

$$\pi^* = 2(S-W)^* + K_1 R^* \tag{2B}$$

$$\frac{dW^*}{dt} = K_6 R^* + K_7 \pi^* + K_8 W^* + K_9 V^* + K_{10} W^* + K_{11} \alpha^* \tag{3B}$$

$$(S-W)^* = -R^* + K_2 W^* + K_3 V^* + K_4 \gamma^* + K_5 \alpha^* \tag{4B}$$

$$\frac{dV^*}{dt} = K_{12} \pi^* + K_{13} \gamma^* + K_{14} V^* + K_{15} \alpha^* \tag{5B}$$

$$U^* = K_{16} W^* + K_{17} V^* + K_{18} \gamma^* + K_{19} \alpha^* \tag{6B}$$

$$\frac{d^2R^*}{dt^2} = K_{20} U^* - K_{21} \frac{dR^*}{dt} - K_{20} R^* \tag{7B}$$

The coefficients K_i are functions of the geometrical conditions and the initial steady-state conditions. They are relatively long expressions, but for each set of conditions the K_i's are constants.

Preliminary Results

The analytical model was applied to the VBWR core, and stability solutions at various power levels and flow conditions were obtained by analog computer techniques. The model is capable of simulating two types of instability or oscillatory behavior:

1. Loop Oscillation or Instability - The entire core acts as a unit or individual element in series with the external or recirculation loop. The external loop and reactor core oscillate as a system.

2. Parallel Channel Oscillation or Instability - In this case the external loop operates in a steady-state, but, within the core there is superimposed on the steady state flow condition an oscillating flow component. The loop for this oscillating flow is formed by two elements of the core; the flow being in opposite directions at any given instant of time. The elements of this loop, as mentioned above, may be formed by single fuel elements, groups of fuel elements, leakage paths around the core, or any flow path. This type of oscillation was evident in the two-region core described in Section 1 above.

* Indicates normalized form

Instability, as presented used, is simply defined as non-steady conditions and includes oscillations. The term divergent instability or divergent oscillation will be used to indicate oscillations of continuously increasing amplitude.

The stability solutions from the analog model showed that:

1. The loop type oscillation was very stable since it was highly damped by the pipe and valve losses.

2. Parallel channel oscillations could occur since the fuel elements are underdamped, that is, the friction forces are relatively small.

The significance of the second result is that small disturbances to the reactor conditions will cause relatively large oscillations of neutron flux. For random disturbances the magnitude of the system response (flux, inlet velocity, etc.) will depend on the magnitude of the disturbance, just as in any vibrating system the amplitude of vibration is determined by the magnitude of the driving force.

The exact nature of the disturbance or driving excitation that occurs within the reactor is not known at present, but future measurements with in-core instrumentation will be used to evaluate these disturbances. Some of these disturbances may be:

1. Temperature fluctuations at core inlet

2. Pressure pulsations across core due to unsteady level of water above core

3. Statistical non-uniformity of boiling process.

The analytical model predictions will aid in locating the source by indicating the different character of response to various impulses. For example, as a function of increasing power level, the table below gives the disturbance and response:

Disturbance	Response With Increasing Power Level
Inlet temperature	Flux amplitudes increase
Pressure drop across core	Flux amplitudes exhibit a minimum
Flow	Flux amplitudes decrease

Another prediction of the analytical model is that the resonant oscillation frequency increases as flow rate and power increase. The preliminary results in Figures 10 and 11 seem to confirm this prediction.

The preliminary experimental tests have served to demonstrate the reactor behavior, perfected data gathering techniques, and oriented the analytical and calculational programs.

E. Task A-VI Irradiation in VBWR

The work in this sub-task is concerned with the irradiation of the Fuel Cycle fuel in VBWR. Specifically, this includes VBWR start-up tests, fuel-life tests on the Fuel Cycle fuel and reactor performance tests. The critical tests were done with the ten stainless steel clad fuel follower assemblies in the core and the start-up tests have used the 10 fuel followers plus 15 stainless steel clad fuel-life fuel assemblies.

1. Irradiation History

The maximum power reached so far has been 20 MWT and the average power was about 15 MWT. Figure 16 shows the cumulative total energy in megawatt (thermal) days extracted from all of the fuel in VBWR. Table 3 gives the burnup for each of the fifteen Fuel Cycle fuel assemblies. These values of burnup are based on an average weight of 7.88 kilograms of uranium in the fuel follower assemblies and 9.77 kilograms of uranium in the fuel life assemblies.

TABLE 3

Burnup Per Assembly to January 29, 1961

Assembly No.	Type of Assembly	Burnup (MWD/T of Uranium)
AEC 1H	Fuel Follower	362
AEC 2H	Fuel Follower	323
AEC 3H	Fuel Follower	400
AEC 4H	Fuel Follower	479
AEC 5H	Fuel Follower	362
AEC 6H	Fuel Follower	384
AEC 7H	Fuel Follower	416
AEC 8H	Fuel Follower	412
AEC 9H	Fuel Follower	448
AEC 10H	Fuel Follower	390
AEC 1I	Fuel-Life Fuel	374
AEC 2I	Fuel-Life Fuel	439
AEC 3I	Fuel-Life Fuel	465
AEC 4I	Fuel-Life Fuel	392
AEC 5I	Fuel-Life Fuel	432
AEC 6I	Fuel-Life Fuel	450
AEC 7I	Fuel-Life Fuel	410
AEC 8I	Fuel-Life Fuel	381
AEC 9I	Fuel-Life Fuel	435
AEC 10I	Fuel-Life Fuel	433
AEC 11I	Fuel-Life Fuel	459
AEC 12I	Fuel-Life Fuel	402
AEC 13I	Fuel-Life Fuel	447
AEC 14I	Fuel-Life Fuel	391
AEC 16I	Fuel-Life Fuel	407
	Average	412

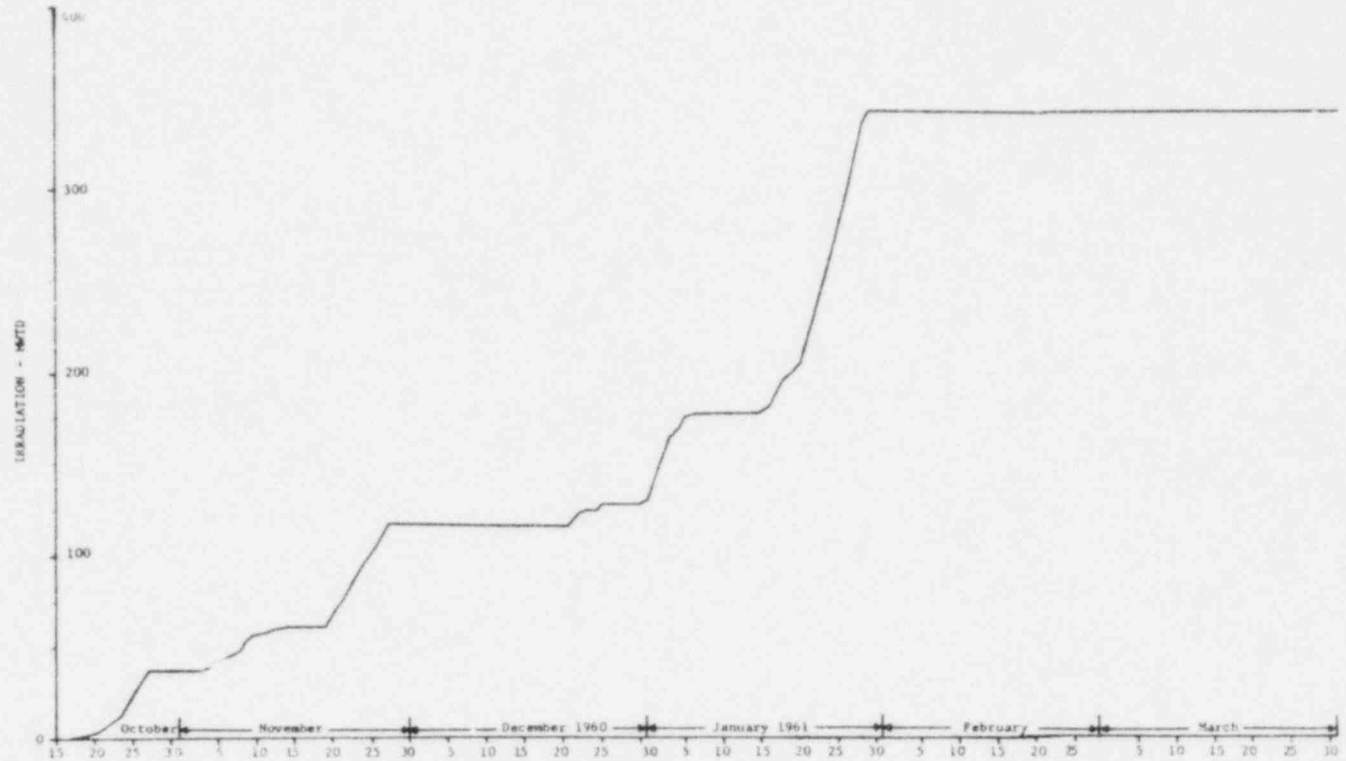

Figure 16

Cumulative Energy (Megawatt Thermal Days)
Extracted From All Fuel in VBWR

The average and peak specific powers achieved in the Fuel Cycle fuel are given in Table 4. These numbers are based on 20 MWT operation in VBWR and with assumed fuel lengths of 29 inches for type H fuel assemblies and 36-inches for Type I assemblies.

TABLE 4

Specific Powers and Power Densities in Fuel Cycle Fuel
(January 29, 1961)

Fuel Type	Average	Peak
Type H	36.0 KW/liter	43.1 KW/liter
Type I	38.4 KW/liter	42.4 KW/liter
Types H & I	28 KW/kg	52 KW/kg

2. VBWR Start-up Tests

During January 1961 the VBWR start-up tests continued. The reactor was brought step-wise up to 20 MWT. The tests performed under the start-up test program were:

a. Transient tests at 9 and 17 MWT
b. Reactivity versus recirculation flow at 9 MWT.
c. Measurements of enclosure and area radioactivity levels at 9 and 17 MWT.

3. VBWR Shutdown

The VBWR was shut down from January 29, 1961 to April for replacement of all the 17-4 PH stainless steel in the core structure and control rod drive shafts.

Recent experience with this material has indicated that at the heat treatment used (900° F) Armco 17-4 PH stainless steel is susceptible to stress corrosion in the boiling water reactor atmosphere. A program of periodic inspection was planned for the control rod drive shafts in VBWR and certain limitations were imposed upon the operations of VBWR to minimize the effect of failure of the in-core components made of this material. A reactor shutdown was planned for about the middle of February 1961 to replace the 17-4 PH components. However, during the inspection of the control rod drive shafts on January 29, a crack was found in the shaft for control rod number 5. The replacement of all the affected parts was begun on January 30.

During the shutdown the vessel head was removed and personnel worked inside the reactor vessel on a 2-inch lead platform suspended as low as 4-inches above the top of the fuel channels. See Figure 4. The fuel had been removed and the vessel water level was just under the platform. Radiation exposure rates were 250 mr/hr at the center of

the platform and 400 to 600 mr/hr between the edge of the platform and the inside of the vessel wall where the work was performed. This is a significant milestone in reactor repair experience.

During the shutdown the Fuel Cycle fuel was given a visual inspection (after approximately 400 MWD/T burnup). All fuel was found to be in good condition. One stainless steel-clad fuel follower fuel rod (from assembly 2H) was discovered to have a white deposit in several spots. A stainless steel-clad corner rod from assembly 4H had two areas of discoloration which suggested that the rod may have run at a higher temperature in these areas than in the surrounding areas of the rod. Closer examination revealed that the integrity of the clad was not diminished by the spots and the decision was made to continue irradiation of the two fuel rods. Figure 17 shows photographs of the assemblies made remotely in the VBWR fuel storage pit.

4. VBWR Loading and Operating Schedules

The following loading and operating schedules assume that approval to operate VBWR is received from the Commission by April 10, 1961.

Table 5

VBWR Loading Schedule
Second Quarter 1961

Program	April 15	May 30	June 30
Dresden	16	17(a)	17
Savannah I	3	3	3
Savannah II	5	5	5
Cellular Plate Elements	2	2	2
Consumers HPD	24	31(b)	32(c)
AEC Fuel Cycle	25	25	25
SADE	1	1(d)	1
Total Test Assemblies	76	84	85
APED Drivers	31	23	22
TOTAL	107	107	107

(a) Add advance Dresden Assembly DP-74.
(b) Add Consumers HPD special elements 3S, 4S, 6S, 7S, 8S and instrumented assemblies 6E and 2F.
(c) Add Consumers HPD special element 9S.
(d) Add SADE I, remove SADE IVb.
(e) Add Fuel Cycle special assembly L-1 and L-6; remove two stainless-clad assemblies.

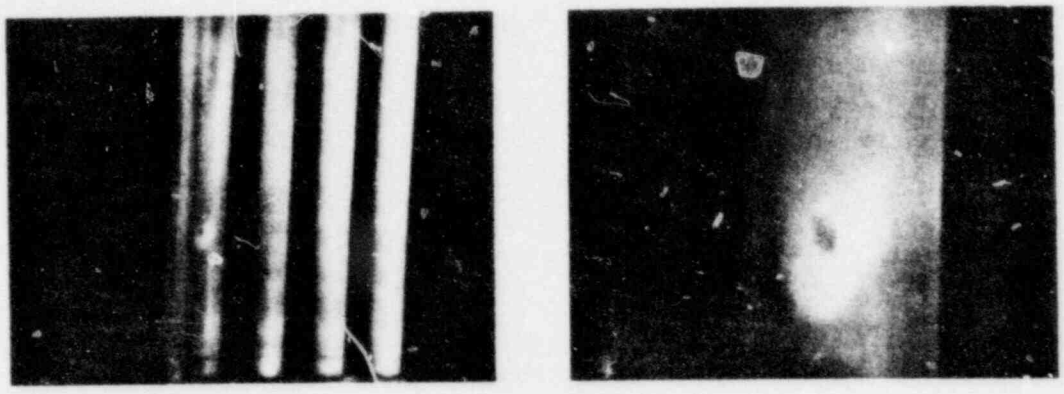

Figure 17a Fuel Assembly 4H After 479 MWD/T

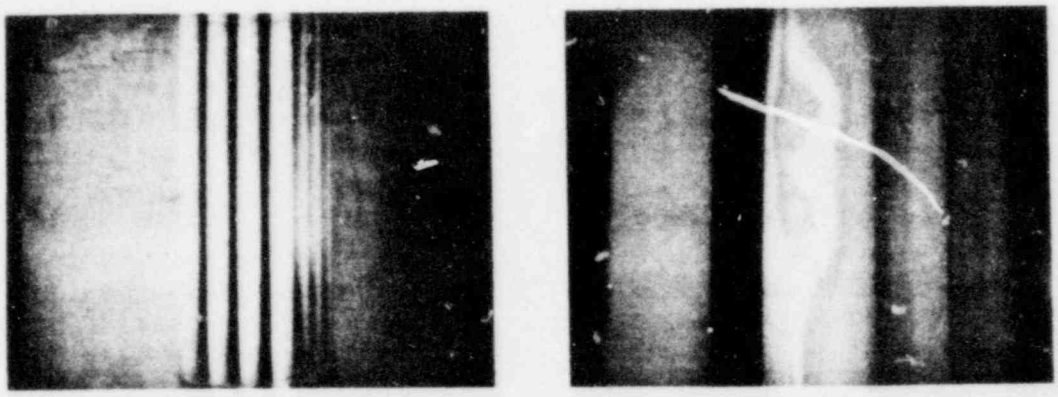

F. Task A-VII Special Fuel Program

In addition to the fuel-life fuel, twelve special fuel assemblies will be designed, fabricated and irradiated in VBWR. The objective of this program is a performance demonstration of fuel concepts not used in current designs of UO_2 fuel.

On January 13, 1961 a meeting was held which included representatives of the Commission and General Electric Company. Participants in the meeting were Messr's M. J. Whitman, G. F. Helfrich and C. V. Backlund of the Commission and Messr's W. H. Cook, K. Kelty and T. J. Pashos of General Electric. During this meeting agreement was reached on the scope of the first eight assemblies of the special fuel program. The fabrication of the latter four assemblies will occur during fiscal 1962.

1. Detailed Description of the Special Fuel Assemblies

A brief description of the fuel concepts to be tested was given in the Second Quarterly Report, GEAP-3627. A more complete description of the fuel assemblies is given below:

a. Fuel Operated in the Centermelt Condition

Assembly No. 1 - An eight-rod assembly with 0.515" O.D., 20 mil stainless steel 304 clad, 5 mil gap, and 0.470" UO_2 pellets of 4.3% and 3.9% enrichment.

This will be used initially for a calibration run for correlation between rod diameter, specific power, and degree of center melt to determine core location and the target for degree of center melting in the other two assemblies.

Assembly #2 and #3 - Sixteen-rod assemblies in a 4 x 4 array with 0.415" O.D., 20 mil stainless steel 304 clad, 5 and 15 mil gap, 0.370" pellets with 3.9% and 5.5% UO_2 pellet enrichment. These two assemblies will operate at two flux levels depending on the calibration results. One rod from each assembly will be run with a one-hole defect.

At approximately every 5,000 MWD/T, one or two rods from the above assemblies will be examined for dimensional changes, fission gas release, and UO_2 void formation, redistribution and recrystallization.

b. Fuel of Higher than 97% Theoretical Density

Assembly No. 4 - A sixteen-rod assembly in which the four corner rods will contain UO_2 fuel pellets of 3.9%

Table 6

VBWR Operating Schedule
Second Quarter 1961

Days After Commission Approval	
0 - 9	Load core, make pre-operational checks and measurements.
10 - 19	Start-up; Make hot critical tests and complete 30 MW Nuclear Start-up Tests.
20 - 27	Full power, steady-state operation.
28 - 31	Shutdown: Charge one Dresden and five Consumers elements. Install flux wires, repair steam leaks.
32	Flux wire irradiation
33 - 40	Shut down; Install prototype B_4C control rod and two instrumented assemblies, remove flux wires, move new assemblies to final desired power locations in core.
41 - 62	Operate steady-state, full power.
62 - 66	Add SADE defect element SADE I, one Consumers HPD special element and two Fuel Cycle special development assemblies.
67 - 90	Operate SADE defect test.

enrichment. At least six of the remaining two rods will be fabricated by the hot gas isostatic pressing process on 5.5% enriched UO_2 fuel and 0.400 inch O.D. by 0.015 inch thick wall cladding. In the hot gas isostatic process UO_2 fuel powder is inserted into its cladding and compressed to a high density by a hot gas. This system was developed by Battelle Memorial Institute.

Assembly No. 5 - A sixteen-rod assembly in which the four corner rods will contain UO_2 fuel pellets of 3.9% enrichment. At least six of the remaining 12 rods will be fabricated with the co-extruded process. In this process the UO_2 fuel is co-extruded with its stainless steel cladding. This process is in development at Nuclear Metals Inc.

These assemblies will be operated at approximatley the same specific power level as the center melt assemblies for a direct comparison. Both assemblies, with higher fuel density than the center melt test pellets and with no diametral gap clearance, should have little or no center melting. Both assemblies will be run to a target peak burnup of 15,000 MWD/T and inspection at 5,000 MWD/T intervals is planned.

c. Fuel with Variations in Cladding

Assembly No. 6 - will be a 16 rod assembly in a 4 x 4 array with 12 rods of 0.370" UO_2 of 3.0% enrichment, clad with a zirconium-niobium alloy. This material may have better corrosion and strength properties than zircaloy-2 or -4.

Assembly No. 7 - will be similar to assembly No. 6 with a cladding of co-extruded zircaloy with a stainless steel lining. The zirconium will be 15 or 22 mils with a 1/2 mil nominal stainless steel lining.

Assembly No. 8 - will be similar to the above with the 12 rods of thin stainless steel cladding. This clad will be 5 to 8 mils in thickness.

One rod of each type of assembly has a defect hole in the clad planned. One or more rods will be removed every 5,000 MWD/T for measurements of dimensional stability, fission gas release, and irradiation effects on the UO_2.

d. UO_2 Fuel with Material Added to Promote Higher Conductivity - Two Assemblies

These assemblies will have 0.370" diameter fuel with 5 mil (and possibly more) gap clearance. Cladding will be 20 mil stainless

steel 304. Here again 12 of the rods will be of fuel with conductivity promoters, with the four corner rods of the 4 x 4 array of 3.9% UO_2 pellets. The enrichment of the fuel with conductivity promoter will be between 6.6% and 6.9%.

Assembly No. 9 - will be UO_2 fuel with molybdenum fibers a process under study by ANL-Armour jointly, Numec, and several others.

Assembly No. 10 - will be of metallic coated UO_2 particles, using a metal such as niobium, a process under development at BMI.

e. Assemblies Not Yet Firmly Defined - Two Assemblies

The objective of these two assemblies will continue to be improved thermal performance, or improved fuel cycle economics.

These assemblies may consist of long UO_2 fuel extrusions, or an alternate material to the uranium oxide fuel, such as uranium nitride.

2. Progress on Procurement of Material for the Special Fuel Assemblies

Table 7 presents a list of the material ordered for the special fuel assemblies and Table 8 gives the present status of the procurement of the material.

TABLE 7

Fuel and Cladding Placed on Order for

Special Fuel Assemblies

Item	Quantity	Remarks	Delivery Date
UO_2 ceramic grade powder	10.0 kilograms	4.3% Enrichment	March 1, 1961
	63.1	5.5%	
	60.1	3.9%	
	49.6	Natural Enrichment	
	27.2	5.0%	
	16.2	6.6%	
	16.2	6.9%	
	19.6	8.0%	
	12.5	10.0%	
UO_2 fused grade powder	26.0	Natural Enrichment	March 31, 1961
304 S.S.; 0.425" O.D. x 0.013" wall x 28" min. lengths	60 ft.		March 1, 1961
304 S.S.; 0.475" I.D. x 0.020" wall x 40" min. lengths	60 ft.		
304 S.S.; 0.375" I.D. x 0.005" wall x 40" min. lengths	75 ft.		
304 S.S.; 0.375" I.D. x 0.020" wall x 40" min. lengths	700 ft.		April, 1961
Zr-2 (0.022" wall) coextruded with 304 S.S. (0.0015" wall); 0.424" O.D. x 0.377" I.D. x 40" long.	20 pieces		

TABLE 8

Status of Material in Special Fuel Program

Assembly No.	Assembly Name	Source of Fuel	Status of Fuel	Source of Clad	Status of Clad
1	Calibration Assembly	N.S. Savannah Project (if permission is received from the Commission)	A letter has been written from GE to the Commission requesting permission to transfer pellets of UO_2 of 3.9 and 4.3% enrichment. This letter includes the needs of the Fuel Cycle Program and an inventory of the fuel available. 13 Kg of 4.58% enriched material may be available from other AEC programs within GE.	Vendor	No delay expected in this assembly because of clad delivery.
2	Centermelt Assembly	Vendor	Estimated delivery June 15, 1961	Vendor	No delay expected in this assembly because of clad delivery.
3	Centermelt Assembly				
4	Isostatic pressed UO_2 Assembly	Vendor	Ceramic grade powder delivery estimated April 1961. Fused grade powder delivery estimated May 1961.	Vendor	Vendor will ship clad to GE for inspection. GE will send clad to BMI for fabrication of fuel rods.
5	Co-extruded UO_2 in SS Clad	Vendor	Natural UO_2 crushed pellets shipped late in March, 1961. Enriched powder has been blended, is being analyzed by GE, and will be shipped to NMI late in April, 1961.	Vendor	No delay expected because of clad delivery.
6	Zr-Nb Clad UO_2 Assembly	Vendor	Transfer of 3% blended powder from license to station status has been requested from the Commission.	Vendor	Clad material is on hand. Must be cut to size and heat treated.

Table 8 Continued

Assembly No.	Assembly Name	Source of Fuel	Status of Fuel	Source of Clad	Status of Clad
7	Zr. Clad Co-extruded with SS Lining	Vendor	Estimated delivery June 15, 1961	Vendor	SAN office suggests that vendor (NMI) fabricate clad under existing AEC contract with NYOO, with Fuel Cycle Program acting as sponsor. This results in estimated schedule slippage of four weeks.
8	Thin SS Clad	Vendor	Estimated delivery June 15, 1961	Vendor	5 to 8 mil stainless steel clad on order. Expect clad approximately April 15.
9	UO_2 Fuel Impregnated With Molybdenum Fibers	Vendor	Details of working agreement not firm with vendor	Vendor	Not ordered
10	Metallic-Coated UO_2 Particles	Vendor	Details of working agreement not firm with vendor	Vendor	Not ordered

IV TASK B - HEAT TRANSFER AND FLUID DYNAMICS

The in-core testing done in Tasks A and C are being supplemented by out-of-pile measurements under Task B in critical areas of heat transfer and fluid flow. This work is aimed at developing more precise correlations and gaining understanding of the phenomena involved. The work also includes extension of the range of data available.

A. Task B-I Burnout Heat Transfer

1. Previous Burnout Work

The objective of this sub-task is to accumulate and analyze additional burnout data to accurately establish the burnout limit of the high-specific-power fuel used for the tests in VBWR. A parallel effort will be made to raise the burnout limit.

Burnout data have been taken in two test sections using an annular flow path and a single cylindrical heater element. The burnout curves taken from the old single rod test section were previously published in the First Summary Report, GEAP-3516. This data showed the trends of the burnout heat flux as a function of mass flow rate, pressure and exit steam quality. Further data was obtained by using the old single-rod test section and was reported in the First Quarterly Report, GEAP-3558. This data compared burnout heat flux under uniform axial heat generation rate to that obtained with a cosine axial heat generation rate. Further data was presented in the Second Quarterly Report, GEAP-3627 which was obtained from the new single rod test section. This latter data again examined the effects of coolant mass flow rate and exit steam quality on the burnout heat flux.

2. New Burnout Data

During the reporting period a study was made of the effect of exit steam quality, mass flow rate, hydraulic diameter and heated length on the burnout heat flux. Existing burnout data was extended to the low steam qualities. These investigations will be continued in the next quarter.

The data upon which the results are based were all obtained in the single rod test section, described in the First Quarterly Progress Report (GEAP-3558, August 1960 - September 1960). It is suitably instrumented to measure total mass flow, system pressure, inlet temperature, and total power supplied to the heated rod. It is also instrumented to detect incipient burnout by sensing a sudden and substantial rise in temperature in the region where burnout would be expected to occur. For uniformly heated rods this region is at the exit end of the rod.

The data permits calculation of heat flux, quality, and flow rate under conditions of incipient burnout. Each parameter can be varied independently of the others, and thus its effect on burnout can be

determined. The results presented in each of the following figures show the effect of varying the exit steam quality plus one other parameter.

Consider first the effects of exit steam quality, x, and mass flow rate, G (lb/hr-ft^2). In Figure 18 the burnout heat flux has an inverse relationship to steam quality. It is also apparent that the burnout heat flux also varies in some inverse manner with flow rate. Note that even in the "negative quality", or subcooled region (i.e., down to -5% steam quality or 26.3° F subcooling) the higher flow rate gives the lower burnout heat flux. This is contrary to the Jens and Lottes correlation (ANL-4627) and the Westinghouse correlation (WAPD-188).

Consider next the effects of exit quality, x, and hydraulic diameter, Dh (inches). In Figure 19a, for a heated length of 9-feet, the burnout heat flux varies in some inverse manner with the hydraulic diameter. However, in Figure 19b. for a heated length of 6-feet, this is not borne out. Figures 20a and b present the same data, cross plotted to show the effects of heated length on the burnout heat flux for constant hydraulic diameter. The same conclusions can be drawn. When the hydraulic diameter is 0.500 inches, the slope of the best fit curve decreases (becomes more negative) as the heated length increases. However, when the hydraulic diameter is 0.335 inches the inverse is true. In the Second Quarterly Report, GEAP-3627, the heated length of rod was described as having "no change---within experimental error". It is evident that the effects of hydraulic diameter and heated length on the burnout heat flux need further study.

3. High-Pressure Observational Boiling Experiment

A parallel effort is being made to understand the heat transfer and fluid dynamics process at the burnout point. High speed photographic data were obtained at burnout in the range of pressure, flow rates, steam qualities and heat fluxes of interest to boiling water reactor technology. These data are intended to provide a basis for theoretical prediction and understanding of burnout phenomena.

a. Summary of Current Results

The experimental phase of this investigation was completed April 14, 1961. The experiment has been operated on an average of about two days per week since start of the final experimental phase the first week of January, 1961. Emphasis has been on obtaining burnout data together with high speed motion pictures of the flow process synchronized with the inception of burnout as well as at lesser heat fluxes and coolant enthalpies.

Figure 21 shows a general view of the final experimental set-up in the General Electric-APED, Building G heat

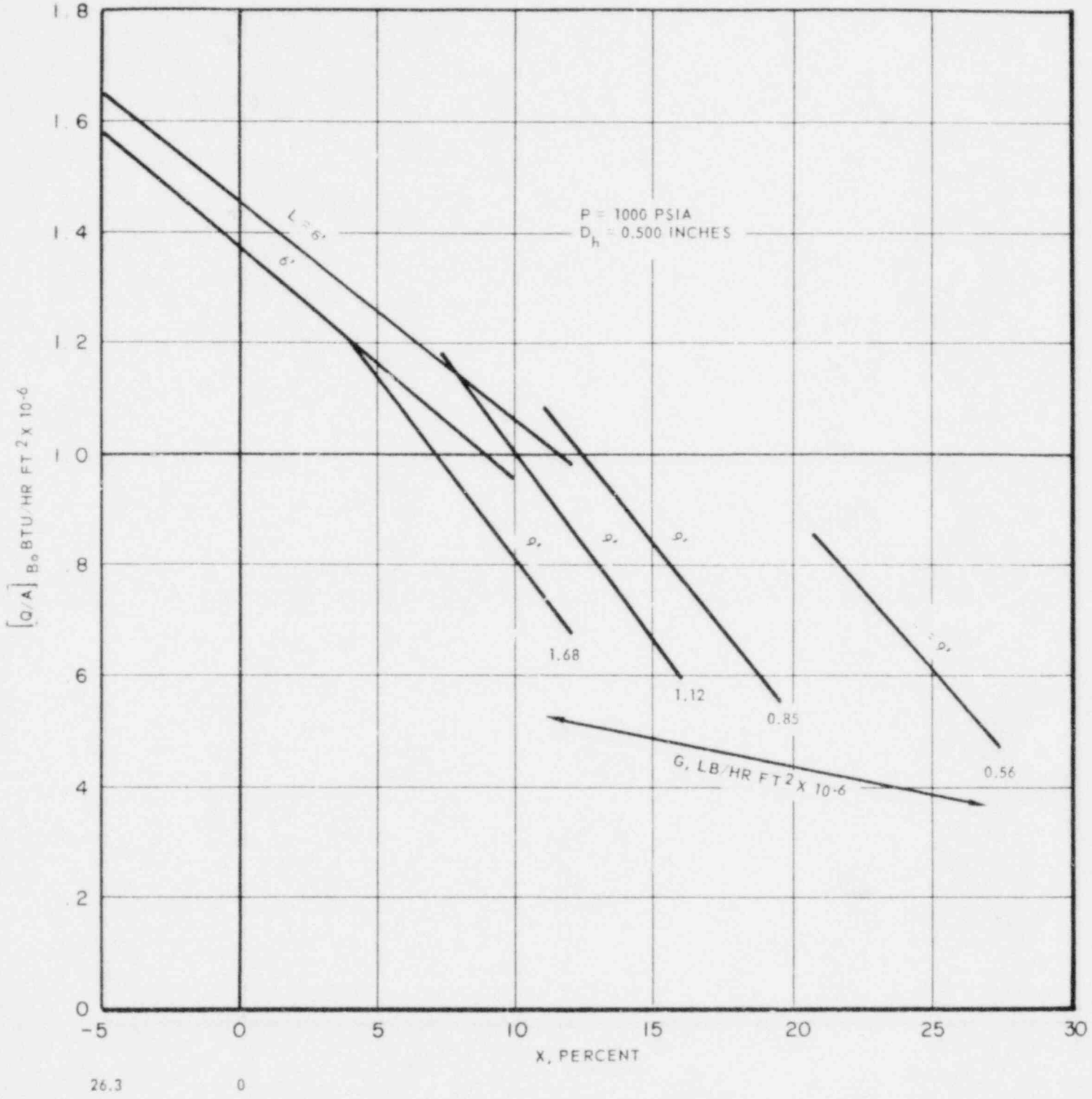

FIGURE 18

EFFECT OF STEAM QUALITY AND MASS FLOW RATE ON BURNOUT HEAT FLUX

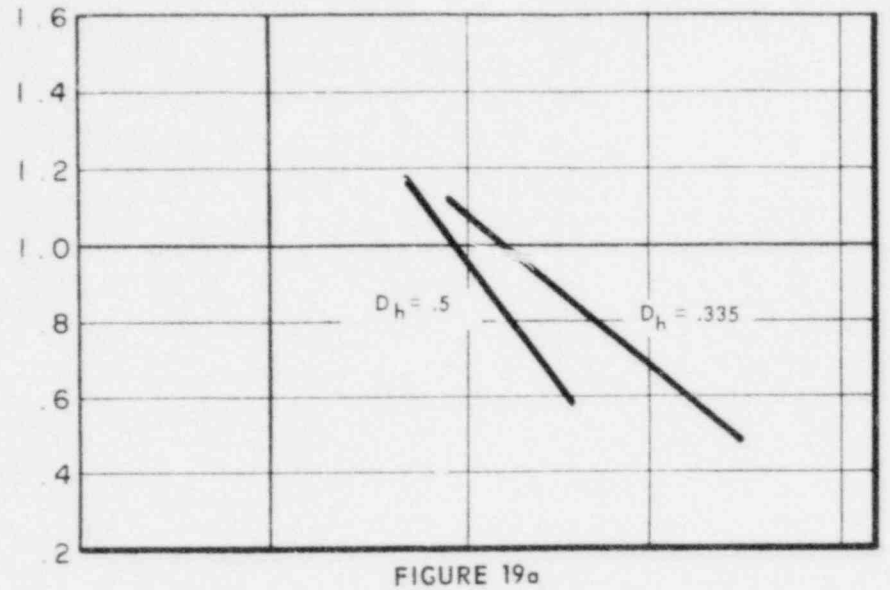

FIGURE 19a

HYDRAULIC DIAMETER EFFECT ON BURNOUT FOR A 9 FOOT HEATED LENGTH
PRESSURE = 1000 PSIA
G = 1.12 x 10^6 LB/HR-FT^2

$[q/A]_{BO}$ BTU/HR FT^2 X 10^{-6}

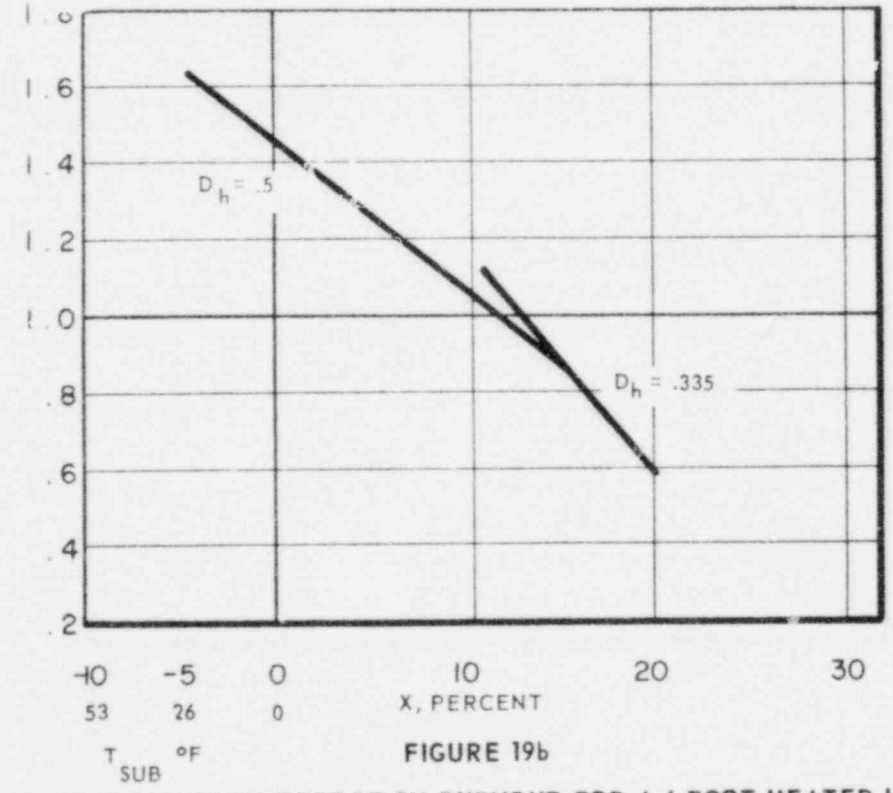

FIGURE 19b

HYDRAULIC DIAMETER EFFECT ON BURNOUT FOR A 6 FOOT HEATED LENGTH
PRESSURE = 1000 PSIA
G = 1.12 X 10^6 LB/HR-FT^2

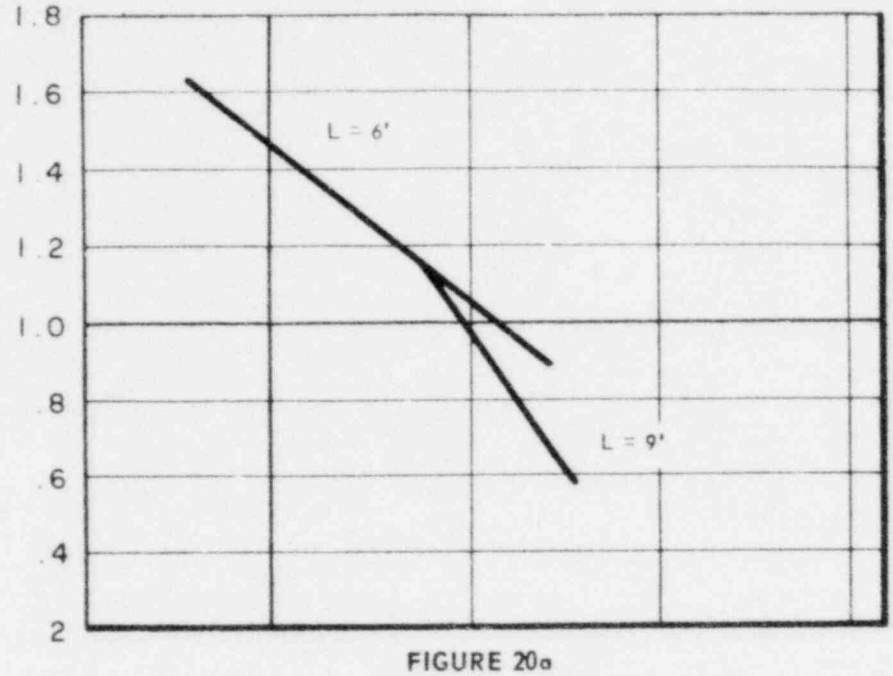

FIGURE 20a

HEATED LENGTH EFFECT ON BURNOUT FOR 0.500 INCH HYDRAULIC DIAMETER
PRESSURE = 1000 PSIA
$G = 1.12 \times 10^6$ LB/HR-FT^2

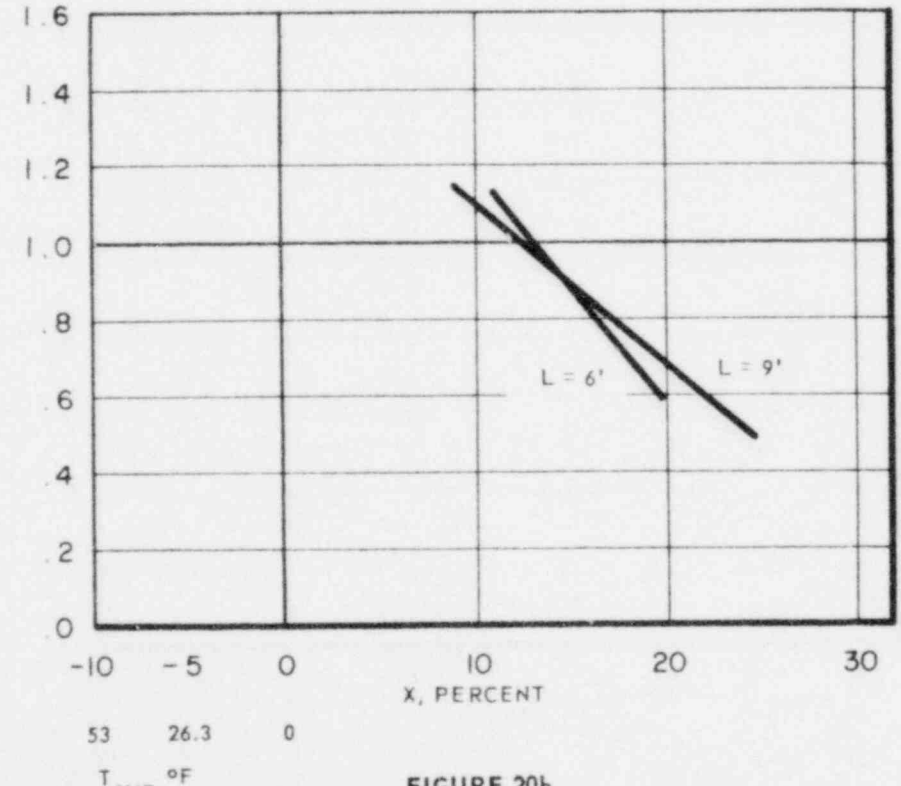

FIGURE 20b

HEATED LENGTH EFFECT ON BURNOUT FOR 0.500 INCH HYDRAULIC DIAMETER
PRESSURE = 1000 PSIA
$G = 1.12 \times 10^6$ LB/HR-FT^2

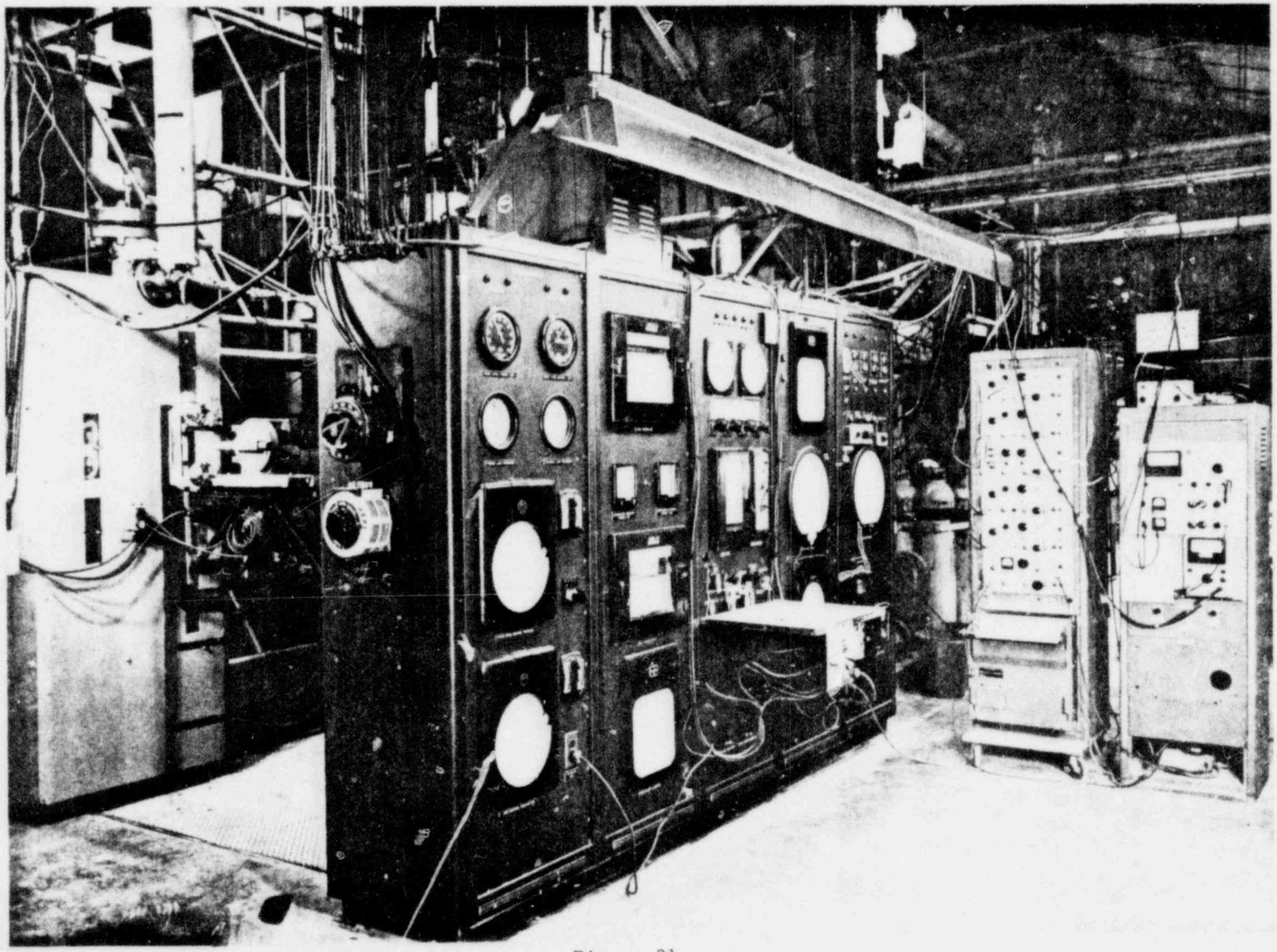

Figure 21

General View of Experimental Equipment
in High Pressure Observational Boiling Experiment

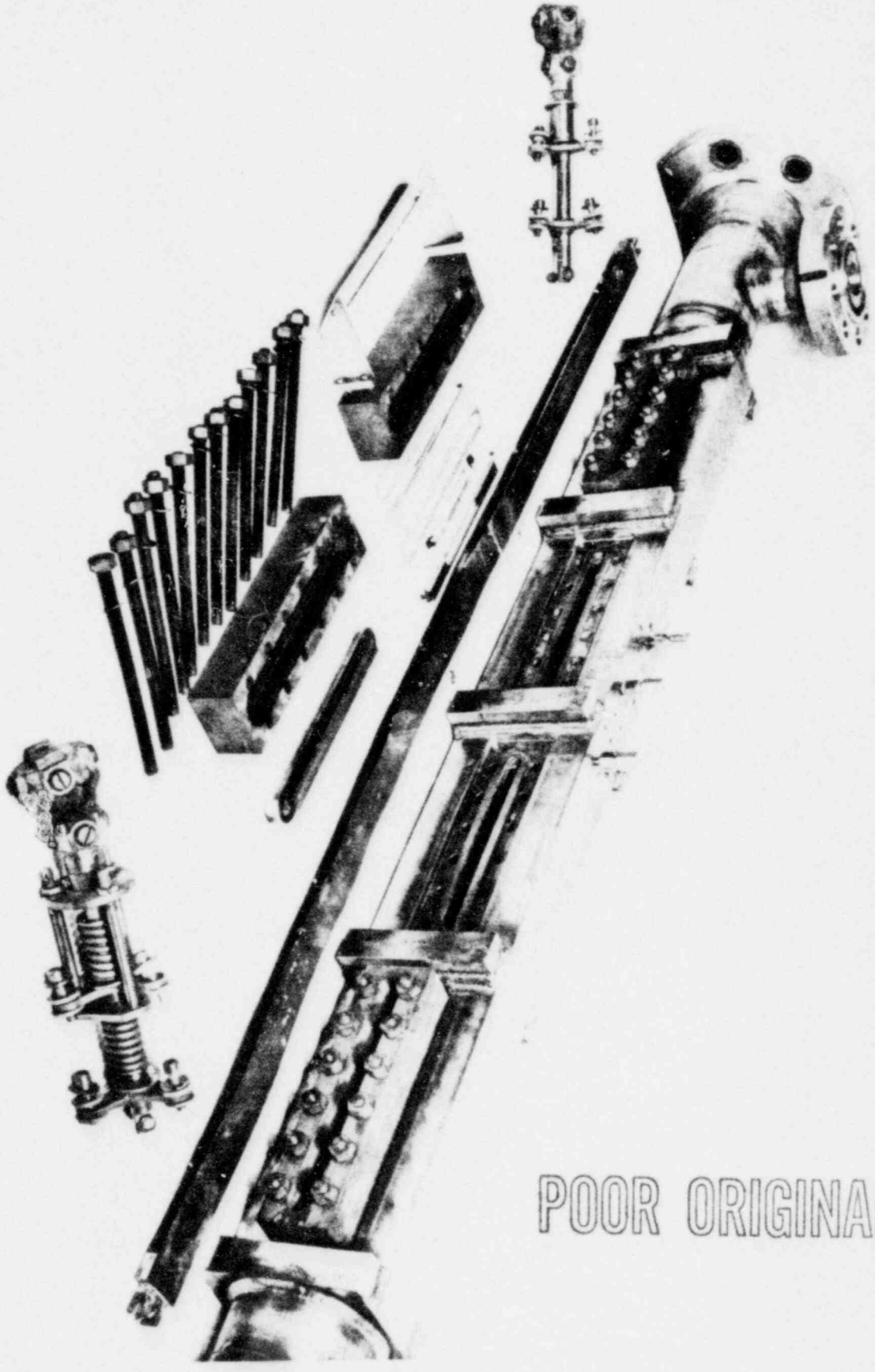

Figure 22

Principal Parts of Observational Test Section

transfer test facility. The high pressure observational test section is in its safety enclosure with camera and lights in the left background. The system control and instrumentation equipment is in the foreground. Figure 22 shows the principal parts of the test section. These include the flat plate heater element, the photographic window assembly and optical viewing mirror. Figure 23 shows a used heater element after a typical "actual burnout", in comparison with a new element.

All equipment and instrumentation problems associated with this new experimental facility have been adequately solved, including:

(1) refinement of the heater element design and fabrication technique,
(2) development of the special pyrex glass - crystalline sapphire photographic window,
(3) refinement of the high speed photography technique, camera and lens settings, lighting, and film processing,
(4) development of special burnout detection instrumentation to prevent heater element destruction and to provide a means for synchronization of the high speed movie camera and lights with the inception of burnout.

The following range of experimental conditions have been covered with repeated burnout points. A set of high speed motion pictures were taken at each of the several combinations.

Table 9

Range of Variables in the Observational Boiling Experiment

Pressure	985 - 1015 psia
Mass Velocity	50, 100, 200, 400 lbs/sec. ft^2
Inlet Subcooling (adjusted to vary steam quality)	22 - 215 Btu/lb
Heat Flux (burnout points)	0.60 - 1.16 x 10^6 Btu/hr-ft^2
Exit Steam Quality (burnout points)	0.04 - 0.80

Heater Element:	Length	Width	Plate Spacing	Plate Thickness
(rectangular channel,	41"	1.965"	1/2"	0.010"
2 flat plates cooled	41"	1.965"	1/2"	0.006"
on inner sides)	41"	1.965"	1/4"	0.010"
	41"	1.965"	1/4"	0.006"
	41"	1.965"	1/2"	0.010"*

* One plate only heated.

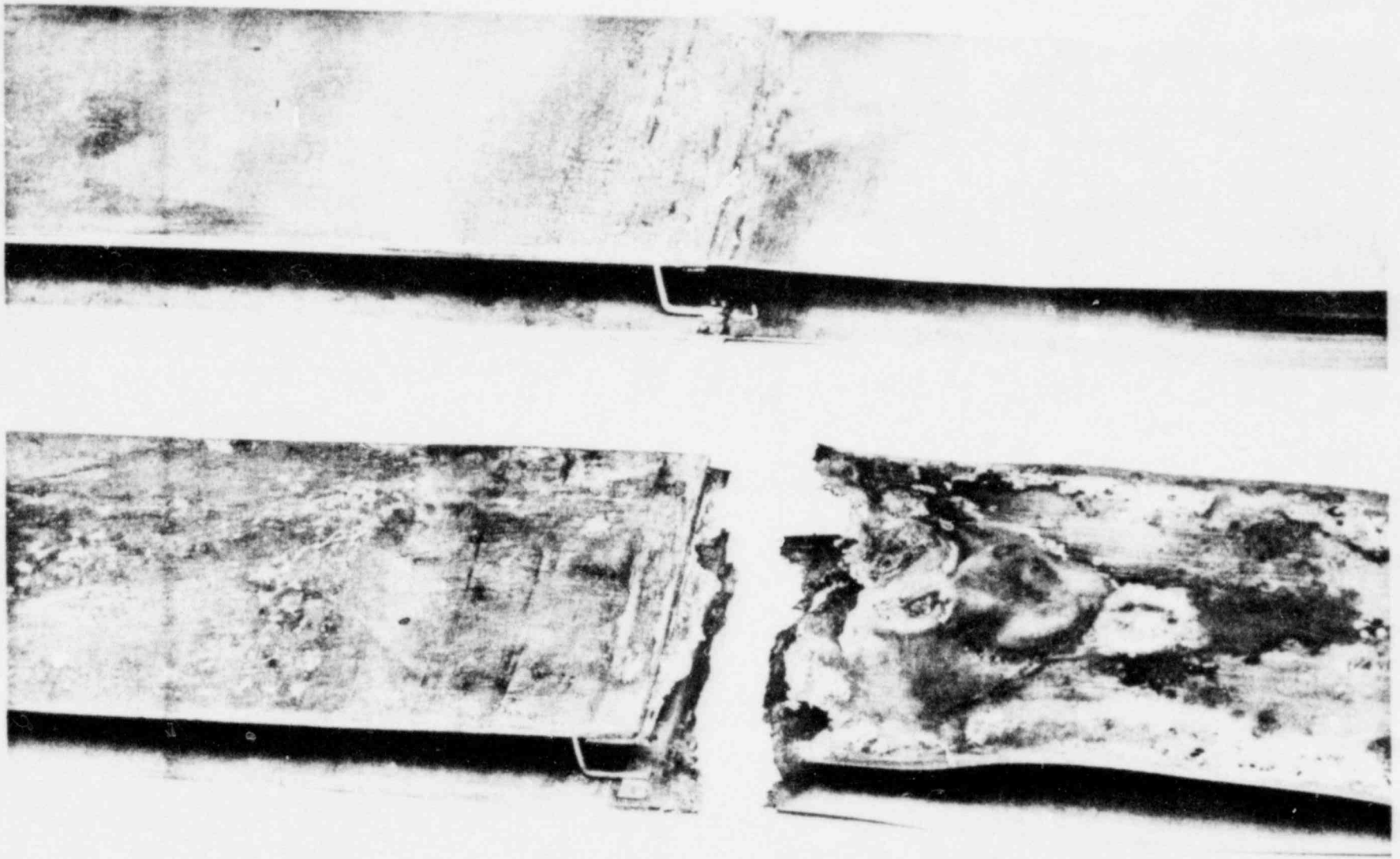

Figure 23

Observational Test Section Heater Elements
Before and After Actual Burnout

This range of operating conditions was covered for burnout runs by means of 32 separate operating set points (fixed flow, inlet subcooling, pressure, and heater element). For each set point, burnout was approached by slowly raising power while holding all other system variables constant until the safety monitor tripped the power supply circuit or, as happened a few times, the heater element physically was destroyed by overheating. Data for a total of 80 valid burnout points, including five actual burnouts, were obtained for the 32 operating set points. Most of the individual set points were covered by two or more repeated burnout runs with the repeats being made sometimes after the elapse of several days or weeks and with different heater elements. Reproducibility of the burnout points is good. For repeats of both "burnout trips" as well as "actual burnouts" the mean heat flux deviation at individual repeated burnout points is less than $\pm$ 1-1/2% over the entire range of data. The maximum deviation of the burnout heat flux at any point is about $\pm$ 5%.

Sets of high speed motion pictures of the flow process were taken at 15 of the operating set points covering the entire range of experimental conditions. The range of fluid enthalpies and heat fluxes for the motion pictures extended from subcooled nucleate boiling at relatively low heat fluxes (250,000 - 500,000 Btu/hr ft^2) up to the burnout trip point at the burnout heat flux and steam quality. A total of one-hundred and six 100 ft. rolls of high speed movie film was exposed, including several trial and test films. Preliminary editing of these indicates that about one-half of them are of acceptable photographic quality and adequately representative of the flow process they were intended to record. For each of the 15 set points covered by the motion pictures, one or more motion pictures was taken either in synchronization with or immediately before the burnout trip point. A total of 28 such movies at the burnout condition were taken. The movies were exposed with a Fastax camera (Model WF-3) operating at approximately 4500 pictures per second. It was equipped with a telescopic lens and extension tube to photograph a 9/16-inch field at the upper end of the heater element where "burnout" occurred. The camera and photographic lights were simultaneously started remotely by a master switch at the control panel. The decision as to when to start the camera in order to synchronize with the burnout point was based upon scrutiny of the character of the Sanborn recorder trace of the safety monitor balance signal as the test section power was raised slowly to the burnout trip point.

The principal effort planned through June 1961 will be on:

(1) final reduction of the burnout data,
(2) editing of the high speed motion pictures,
(3) study and measurement of the hydrodynamics of the two-phase flow process as exhibited by the high speed motion pictures,

(4) theoretical analysis of burnout in bulk boiling based on the detailed flow characteristics exhibited by the high speed movies together with the numerical burnout data obtained in this experiment and in the other heat transfer experiments performed under the AEC Fuel Cycle Program.

A topical report covering the entire investigation, including the design and development of the experimental apparatus and test section, the experimental results, and the theoretical analysis, will be issued in fiscal year 1962 following completion of the theoretical phase. (These results are to be submitted by F. E. Tippets as a doctoral dissertation to Stanford University, Professor A. L. London, faculty advisor.)

b. Review by Professor J. W. Westwater

Professor J. W. Westwater of the Department of Chemical Engineering, University of Illinois, was contracted in January, 1961 to review the experimental setup, operating procedure, and photographic equipment and technique from the standpoint of advisor, consultant and critic. This review was considered to be appropriate in view of Professor Westwater's high reputation as a researcher in boiling heat transfer using special techniques of high speed photography.

The consultation was performed under General Electric P.O. 205-28933-G.

Professor Westwater's report for his consultation visit January 25-27, 1961 follows verbatim:

COMMENTS ON VISUAL FLOW STUDIES
WITH BOILING IN A FLOW CHANNEL*

J. W. Westwater
Professor of Chemical Engineering
University of Illinois, Urbana

I. Present Work

The work on visual flow studies with boiling in a flow channel presently underway at APED in San Jose is of very good quality. Progress has been quite rapid. No obvious blunders or serious errors in the equipment or operating procedure can be listed. A few items may be discussed as shown below.

* Included in letter of February 13, 1961, J. W. Westwater to F. E. Tippets.

1. Window Fouling

The variability in photographic quality of one motion picture film compared to another, for the high pressure tests, may be a result of fouling at the viewing windows. The visibility seems to change by a considerable degree in a period of 12 hours. Fouling ordinarily means the deposition of a foreign material. It would be wise to collect some of the fouling film and have a chemical analysis made. This should furnish clues to permit future decreases in the fouling rate.

Fouling is often very sensitive to dissolved oxygen. It is possible to operate the test loop with oxygen-free water. Oxygen can be removed from water by pre-boiling, by sparging with nitrogen, or by use of chemical scavangers.

Whenever the loop is opened for test-section removal or for maintenance, air enters the piping. Some oxidation of the metal undoubtedly occurs during air contact. After the loop is closed and flow is resumed, what happens to the metal oxides? If they stay in place, no harm is done. But if they are swept off the metal surfaces and redeposit on the windows or on the heat transfer surface, they are highly objectionable. Thought should be given to keeping the entire system free of air even during shutdowns. A blanket of nitrogen, continual storage of oxygen-free water in all the loop, or some other scheme could be used. The complete exclusion of oxygen from the flow system probably is enforced with the Dresden reactor already. Mr. Harry Ongman was concerned with the Dresden water system and should be able to give valuable advice on aspects of water purity.

If fouling is caused by compounds formed by reaction of pure water with the construction materials in the test loop, the exclusion of oxygen will not be a cure-all. In this case a clean-up system should be installed in the loop, probably as a bypass to take a fraction of the flow. The film-formers would be removed continuously in the clean-up device. A clean-up system cannot be selected until the identity of the fouling material is known. If the film-former consists of suspended matter, some of the possible clean-up devices include filters, centrifuges, and magnetic separators. Which is best depends on the size and number of the particles and whether they are magnetic or not. If the fouling material is in true solution, it can be removed by ion exchange beds, by chemical scavengers, or by use of a distillation column.

It is conceivable that loss of visibility at the sapphire windows is caused by direct chemical reaction between the windows and the water or direct solution of the windows in the water. If either is taking place, the problem is most difficult. The only ways to reduce the rate of solution of

a solute in a solvent are to reduce the degree of agitation and to reduce the driving force. The former is out of the question. Possibly the driving force for solution could be reduced. This would call for installing a chamber containing crushed aluminum oxide in the flow stream. Thus the water would be presaturated with aluminum oxide as it entered the test section. Of course as the water passed through the test section its temperature would rise and some solution would still take place. If chemical reaction, rather than simple physical solution, occurs between the water and the windows, pre-contact with crushed window material would still be of help. In this case the existence of dissolved reaction-products would slow down the reaction in accordance with the general principles for reversible reactions.

2. Light Intensity

Possibly the quality of the motion pictures could be improved by use of more intense light coupled with a smaller lens aperture in the camera. At present the lights are used at their rated voltage. They definitely can be operated at an overvoltage. At 130 volts the illumination is appreciably greater than at 110 volts. The chief penalty incurred is a reduction in the life of the lamps. From the cost standpoint the lamp life is a minor item. Of course the aperture can be reduced also if the framing rate is decreased. The framing rate should never be faster than actually needed to measure the action.

3. Size of Field of View

At present the work of Mr. F. E. Tippets includes two sizes for the field of view. This writer felt that the smaller field of view was more informative than the larger. The films of Dr. Earl Janssen with the low pressure loop used several fields of view. The smaller fields again seemed most helpful. If these conclusions are correct, then an even smaller field might be still better. A smaller field can be obtained, without the use of a microscope, by the proper selection of lens, extension tubes, and lens-to-target distance. Of course a smaller field usually calls for a greater light intensity. Item 2 suggests ways of improving this.

If a close-up is used, the entire channel width will not be visible. Films would be needed for several positions across the width, including the edge of the flow channel. A good view of the action at the heat transfer surface is of particular interest.

4. Focal Plane

At present the focal plane is selected to be a definite distance in from the window surface for the high pressure loop. It would be reasonable to try with the focus at the inside surface of the window. This might show the action more clearly. The writer suspects that little improvement would result, but the only way to find out is to try it.

5. Framing Rate

The present framing rate, about 4000 frames per second, is too fast to permit identification of phenomena which occur slowly. If flow oscillations occur at a frequency near one cycle per second, they may not be detectable in the films. Flow oscillations are sometimes evident in the tracings from the flow recorder, particularly as the burnout point is approached. The frequency is in the order of one cycle per second. It should be valuable to obtain motion pictures exactly during flow oscillations. The framing rate should be slow enough to record a number of cycles of the flow oscillations. These films should be taken with a common timing mark both on the film and on the tracing of the flow recorder. This would insure proper synchronization of the two types of data. A study then could be carried out to discover what actually happens in the channel during the so-called oscillations.

II. Future Work

1. View Normal to Surface

The view offered by a camera is a one-eyed view lacking true perception of shapes in three dimensions. If fruitful information is obtainable from profile photography, then additional helpful information would be provided by photography normal to the heating surface. The size and shape of bubbles, drops, and slugs of fluid can be known with certainty only after photography from two angles has been used.

2. Heater Metal

The use of stainless steel or some other alloy is attractive for electrical resistance heating because of the favorable magnitude of the resistance of alloys. However, the determination of the temperature of such heaters is quite difficult, troublesome, and prone to many types of errors.

From the temperature measurement viewpoint the use of pure metals, instead of alloys, for the heater is attractive. A pure metal can be used as a resistance thermometer. Pure

metals have a strong dependence of electrical resistance on temperature. Once a heater made of a pure metal is calibrated, then its temperature during any heat transfer run can be established by measuring its electrical resistance.

Admittedly problems arise when a pure metal is used instead of an alloy. The mechanical strength and the resistance to corrosion of commercial alloys are usually superior to the performance of pure metals. The electrical resistance of a pure metal is less than that of its alloys. Thus a pure metal heater would demand greater electrical current, perhaps by as much as an order of magnitude. Possible metals for consideration are nickel, tantalum, titanium, zirconium, tungsten, platinum, etc. At low temperatures and pressures copper or aluminum may be suitable.

The present work is concerned with a transport phenomenon, heat transfer. The method of measuring the flux is quite good, but the method of getting the driving force is less good. In the future more attention should be given to the driving force.

3. Choice of Liquid

For evaluating the actual performance of water at high temperature and high pressure in long channels, one must actually make tests with water at high temperature and high pressure in long channels. However, if the goal is to conduct basic research, each experiment should be designed to answer a specific question. For example, if we wish to know the effect of varying the ratio of vapor density to liquid density, water is a poor test substance. The ratio could be varied much more easily and without the use of extreme temperatures or pressures by choosing some other liquid such as liquid carbon dioxide. Various petroleum fractions also have critical pressures which are not far from atmospheric pressure. These would be easy to use with a great range in the density ratio.

If we wish to see how flow oscillations depend on the enthalpy change during evaporation, water is satisfactory for one test fluid. But here again water demands great variations in temperature and pressure to result in significant changes in enthalpy. Large relative changes can be achieved more simply by use of other test liquids. Carbon tetrachloride and pentane are good examples. Fire hazard is a detriment, but carbon tetrachloride, the freons, liquid carbon dioxide, and a few others are non-flammable. Flammable liquids are usable, with proper know-how, as demonstrated by daily operations in any petroleum refinery.

4. Size of Test Equipment

The present test loops are large, costly, and slow to operate. All this is necessary when full-size test elements must be evaluated.

However, if basic research is anticipated, small bench-scale rigs become desirable. Possibly 10 or 20 such rigs could be run on a budget such as needed to run one big loop. Many specific questions can be answered rapidly with small rigs. For examples: the effect of dissolved oxygen on fouling rates, the effect of dissolved impurities on the heat transfer rates, and the effect of surface texture on the burnout heat flux. If long-range work is expected, the construction of a number of small test rigs is highly advisable.

B. Task B-IV Two-Phase Pressure Drop

The work in this sub-task includes the measurement of single and two-phase pressure drop in flow geometries of interest to boiling water reactors. At present, the work planned includes the single and two-phase measurements made across a full scale prototype of the Fuel Cycle fuel assemblies and two-phase pressure drop tests through such basic geometries as sudden contractions and expansions. The prototype tests were completed in December 1960. Some of the preliminary results were reported in the Second Quarterly Report, GEAP-3627. A topical report is being prepared.